CoA Memo No 119

THE COLLEGE OF AERONAUTICS

DEPARTMENT OF ELECTRICAL AND CONTROL ENGINEERING

CRANFIELD

C.V.D ANNUAL REPORT : JANUARY, 1967

RESEARCH PROJECT RU27-1

Analogue study of semiconductor device structures

- by -

R. Andrew

and

H.W. Loeb

S U M M A R Y

The extension of the resistance network analogue method to the study of a M.O.S.T. structure is described. By means of an iterative technique, data regarding channel current, field distribution, surface charge and position of pinch-off point as function of gate and drain voltages can be obtained which do not involve the usual 'gradual' channel approximation. Results for a particular device geometry are presented.

A discussion of a digital computer approach to the solution of semiconductor device current flow problems is included, together with preliminary results.

DISTRIBUTION LIST

No. of copies	Addressee
10	DNPR/CVD, Ministry of Defence, Old Admiralty Building, Whitehall, London, S.W.1.
1	Dr. T.S. Moss, RAE, Radio Department, Farnborough, Hants.
1	Dr. P.J. Holmes, RAE, Radio Department, Farnborough, Hants.
1	Dr. J.W. Granville, RRE, St. Andrew's Road, Malvern, Worcs.
1	Mr. G. Avis, SRDE, Somerford, Christchurch, Hants.
1	Mr. G.W.E. Stark, SRDE, Somerford, Christchurch, Hants.
1	Mr. K.G. Hambleton, SERL, Baldock, Herts.
1	Mr. D. Baker, PORS, Dollis Hill, London, N.W.2.
1	Mr. K. Kandiah, AERE, Harwell, Didcot, Berks.
1	Dr. J.R. Tillmann, PORS, Dollis Hill, London, N.W.2.

Contents

	Page No.
Summary	
Introduction	1
Part A - Analogue study of M.O.S.T. structure	2
I - General	2
II - Theory	4
III - The Resistance Network Analogue	11
IV - Results	13
V - A Note on Errors	15
References	16
Appendix A - The Surface Channel Approximation with Diffusion	17
Appendix B - Solution with Approximation of Equations of Electron Fermi Level within the Base Region	19
Part B - A Numerical Method for the Solution of the Semiconductor Current Flow Equations	22
I - General	22
II - The Finite Difference Scheme	24
III - Stability and Convergence	26
IV - The Error Analysis	27
V - The Abrupt p-n Junction	30
VI - Summary	32
References	32

List of symbols

$p(\underline{x})$, $n(\underline{x})$	hole/electron concentration
N_A	acceptor concentration within base
N_D	donor concentration at source and drain contacts.
n_i	intrinsic carrier concentration
j_n	electron current density
J	total channel current
i_g, i_d, i_s, i_b	terminals currents at gate, drain, source and base.
i_s	diode saturation current
$\beta = \frac{e}{kT}$	reciprocal of mean thermal energy per degree of freedom.
ϕ_p, ϕ_n	hole and electron fermi levels.
ϕ	electrostatic potential function
U	voltage
V	potential along semiconductor/oxide interface
V_i	potential of ith node
V_g, V_d, V_s, V_b	terminal voltage at grid, drain, source and base.
e	magnitude of electronic charge
κ_o	permittivity of free space
κ	dielectric constant
μ_n	electron mobility
P, S, D	position of pinch off point, source and drain along oxide/semiconductor interface
L	oxide thickness
q_i	charge on i^{th} node
$q(x)$	charge distribution
h	fundamental mesh spacing
R	fundamental resistance value.

RESEARCH PROJECT RU27-1

An analogue study of semiconductor device structures

Introduction

This report describes work carried out under the terms of CVD Contract RU 27-1 during the period from October 1965 to December, 1966. The presentation is divided into two parts. Part A consists of a detailed description of the application of the resistance network analogue technique to the determination of the potential distribution and channel current flow in a M.O.S.T. device and includes a set of results obtained for a specific device geometry of practical significance.

The resistance network method offers the advantage over other methods of analysis of not being limited to the so-called 'gradual channel' approximation, which was first used by Shockley(1) in 1952 in the discussion of field-effect transistor action and which has formed the basis of practically all published studies of M.O.S.T. devices. On account of this difference, the model to be discussed is believed to constitute a significant improvement on earlier models in spite of the fact that practical limitations of the present resistance network impose a number of restrictions to the accuracy of obtainable solutions.

Part B of this report considers a numerical method for the solution of the equation of current flow in semiconductors in their most general form.(2) The feasibility of the method is discussed. A particular approach to the formulation of a computing procedure of general applicability and preliminary results obtained by its use are presented.

Part A Analogue study of M.O.S.T. structure

I General

The principles underlying the application of resistance networks to the simulation of semiconductor systems in a manner involving the correct representation of the Boltzmann terms governing the electron and hole concentrations as functions of the local potential by means of matched diode groups have been set out in a previous report(3) and elsewhere(4) and will not be repeated here. Essentially, the method permits the investigation of quasi-equilibrium situations (constant quasi-Fermi levels) with a maximum of flexibility and ease of operation but requires procedures of considerably increased complexity if current flow becomes a significant factor in the determination of potential and carrier distributions. In such cases, in addition to the potential, the values of the quasi-Fermi levels at every point in the system have to be found ('complete solution').

The method used in the present investigation represents a compromise between the two extremes of quasi-equilibrium methods and complete solution methods. It is based upon an iterative technique,* described in detail in the following sections, which permits the inclusion of an electron current component along the oxide-semiconductor interface without the necessity of representing electron quasi-Fermi levels explicitly.

The device chosen for the analogue study consisted of a silicon M.O.S.T. structure which is currently under investigation at the Mullard Research Laboratories, Salfords, Redhill. The dimensions of this transistor are shown in Figure 1. The insulating oxide layer of thickness 0.2 microns is formed on a substrate of p-type silicon with a donor concentration, assumed uniform, of $6.7 \times 10^{13} cm^{-3}$. The source and drain contacts, which are taken to consist of heavily doped n-type material, are

---

* This technique was first suggested by Dr. F. Berz of Mullard Research Laboratories, Redhill, Surrey.

in contact with the bulk material along the interfaces shown. The base contact to the bulk material is assumed to be ohmic. The device is of planar geometry leading to a description in terms of the two-dimensional model illustrated. The source-drain separation equals 12 microns.

The mode of operation to be analysed is the basic D.C. mode, characterized by a base to source reverse voltage, hence essentially zero base current, with positive gate and drain voltages. The positively biassed gate will produce partial depletion of holes in the base region adjacent to the oxide-semiconductor interface and will give rise, for sufficiently high gate voltages, to a narrow inversion region along this interface. This provides the electron 'channel' involved in the transport of electrons from source to drain electrode, corresponding to a current of magnitude J. The situation is characterized by the conditions:

$$i_b = 0;\ i_g = 0;\ V_d > V_s;\ V_g > V_b;\ i_s = i_d = J$$

(the subscripts b, g, s, d refer to base, gate, source and drain respectively).

If recombination/generation processes in the base region are neglected then current flow is solely due to the transport of electrons from source to drain. This current flow may be described in outline by appealing to some intuitive knowledge of the field distribution within the device. Thus if $V_g > V_d$, then the field at all points along the silicon/oxide interface will be directed into the base region and thus the flow of electrons will be along a surface channel. But if $V_g < V_d$ then although an inversion layer will be formed near the source, it will 'pinch-off' as the normal field to the surface decreases, and the current near the drain will pass through the bulk material.

As indicated above an exact solution by the R.N.W.A. (Resistance Network Analogue) method for this kind of structure which would involve the simulation of inversion in the channel region as well as of bulk depletion, requires evaluation of hole and electron quasi-Fermi levels at every point,

and is beyond the scope of the present R.N.W.A. In its place use is made of an iterative method to produce a self-consistent potential distribution and surface current flow pattern. This procedure is equivalent to replacing the partial differential equations corresponding to the general current flow situation by a mathematical model which corresponds to the iterative analogue solution procedure. This simplified mathematical model is discussed in Section II. In Section III follows a description of the R.N.W.A. configuration used. The results obtained in this manner for the field distribution within the device and for the drain current/drain voltage characteristics are collected together and discussed in Section IV.

II - Theory

Our model of the device neglects many features which are present in the practical M.O.S.T., since it is felt either that their inclusion does not particularly contribute to the properties of the model, or that the precise details of their mechanisms is not yet clear enough to warrant their inclusion. Thus it is assumed that there is:-

(a) No recombination or trapping within the base.

(b) Uniformity of impurity concentration within the base.

(c) An abrupt transition between oxide and semiconductor regions at the gate.

(d) No surface impurity states at the oxide/semiconductor interface.

II.1. The field equations

Base region

In the absence of base current, i_b, and of recombination, it may be shown that the hole current is everywhere zero. Thus the hole concentration is given by

$$p(\underline{x}) = n_i \exp \beta(\phi_p - \phi(\underline{x})) \qquad (1)$$

where ϕ_p - the quasi-firm level for holes - is constant. The potential distribution within the base, $\phi_1(\underline{x})$ is given by Poisson's equation

$$\nabla^2\phi_1 = \frac{e}{\kappa_1\kappa_0}\left\{N_A + n(\underline{x}) - n_i \exp\beta(\phi_p - \phi_1(\underline{x}))\right\} \qquad (2)$$

The electron current will be divergenceless in the absence of recombination and hole current, thus

$$\underline{\nabla}\cdot\underline{j}_n = 0$$

and if

$$j_n = -e\mu_n n\underline{\nabla}\phi_n \quad \text{and} \quad n = n_i \exp\beta(\phi_1 - \phi_n)$$

then

$$\frac{1}{\beta}\nabla^2\phi_n - \underline{\nabla}\phi_n\cdot\underline{\nabla}\phi_n + \nabla\phi_1\cdot\nabla\phi_n = 0$$

(3) and (2) are the equations to be solved within the base region. They are coupled and cannot in general be solved independently. although it may be expected that an iterative routine involving the alternate solution of (2) and (3), starting from a trial $n(\underline{x})$ might converge, but this would depend upon the effect of the electrons upon the electrostatic potential distribution.

Oxide Layer

The potential distribution within the oxide layer is a solution of the Laplace equation

$$\nabla^2\phi_2 = 0 \qquad (4)$$

It is not necessary to consider the behaviour of the Fermi-levels within this region, the oxide being considered a perfect insulator.

Source and Drain n^+ - regions

These are highly doped and if their junction with the base region approaches an abrupt transition then to a good approximation the potential of these regions is constant and equal to the voltage applied. Due to the high electron concentrations within the regions the Fermi level for electrons may also be considered constant. Thus

$$\phi = U = \text{constant}; \; \phi_n = U - \frac{1}{\beta}\ln\frac{N_D}{n_i} \qquad (5)$$

The equations (5) may be considered as boundary conditions for the solution of (2) and (3) within the base region.

II.2 Boundary conditions

Solution may be restricted to two regions, the base and oxide regions. The boundary conditions are given in terms of the nomenclature of Figure 2. In this figure the bold lines represent surfaces at which the potential is fixed i.e. the device contacts. The boundary conditions pertaining at the remaining surfaces (corresponding to the dotted lines) are as follows:

(i) and (ii):- field $\underline{\nabla}\phi_2$ is tangential to the surface, i.e. $\underline{\nabla}\phi_2.\underline{n} = 0$; this is the condition for no electrostatic flux-leakage.

(iii) and (iv):- these boundaries are artificial since the semi-conductor is homogeneous through the boundary. If $\underline{\nabla}\phi_1.\underline{n} = 0$ then reflection symmetry is chosen about the surface, a case which is reasonable physically.

(v) The usual continuity conditions for electric fields apply at this boundary, i.e.

$$\kappa_2\underline{\nabla}\phi_2.\underline{n} = \kappa_1\underline{\nabla}\phi_1.\underline{n} \; ; \qquad \phi_1 = \phi_2 \qquad (6)$$

The boundary conditions for the electron Fermi level at the source and drain contacts were mentioned in II.1. Along all remaining boundaries shown in Figure 2 the condition $\underline{\nabla}\phi_n.\underline{n} = 0$ will apply; this is the zero current condition.

II.3 General

Exact analytic solutions of the problem in the above form may be ruled out immediately, leaving only methods which involve solving the finite difference formulae of the equations of the system. Even this would be difficult due to the small grid size necessary to adequately represent a channel whose width were many orders of magnitude narrower than the dimensions of the device. This being so the further approximation that the channel be of negligible width has been made. As such the effect of the channel upon the potential distribution is represented as a surface

charge at the oxide/semiconductor interface.

This will be a good approximation for drain voltages at which 'pinch-off' does not occur ($V_G \geq V_D$), but when 'pinch-off' occurs it would seem necessary to represent the electrons in transit between end of channel and drain as bulk space charge. In fact in the analysis this bulk electron charge has been neglected, but it is quite likely that its inclusion would have had little effect upon the results for two reasons. Firstly the mobility of the carriers in the channel will be less than in the bulk material, thus the density of electrons in the bulk will be effectively reduced. Secondly, the current flowing in the channel is space charge limited whence the bulk electron charge would only affect the channel current in so far as it affects the potential distribution along the oxide/semiconductor surface. The model also excludes the effect of diffusion upon the channel current. It can be shown that the neglect of the diffusion component of current, which is a common feature of most of the published work in this field, does not significantly alter the total current. A discussion of this point is presented in Appendix A.

The problem is now in a form that may be solved by the R.N.W.A. The electrostatic potential function must satisfy the same boundary conditions as discussed in II.2 except at the interface between oxide and semiconductor, where the boundary conditions become

$$\text{(i)} \quad \kappa_1 \underline{\nabla} \phi_1 . \underline{n} - \kappa_2 \underline{\nabla} \phi_2 . \underline{n} = \begin{cases} -\frac{1}{\kappa_o} q(x), & x < P \\ 0, & x > P \end{cases} \qquad (7)$$

$$\text{(ii)} \quad \phi_1(x) = \phi_2(x)$$

$$\text{(iii)} \quad \mu_n q(x) \frac{\partial \phi}{\partial x} = \begin{cases} -J, & x < P \\ 0, & x > P \end{cases}$$

Two extra parameters are introduced in the equations (7). These are J - the total current, and P - the pinch off point. Two more boundary conditions are required to fix these parameters for the device in a particular state.

P is fixed by requiring that

$$q(x)\Big|_{x=P} = 0 \qquad (8)$$

A condition for fixing J is more complex and must be equivalent to the continuity of electron quasi-Fermi level at the source. This leads to difficulties since an electron Fermi level is meaningless in the context of the present model. Instead an intuitive condition is applied. At some point along the interface, quite close to the source, the depletion layer will be of minimum width. At this point x_o it is assumed that the normal component of field in the oxide is terminated exactly by the electrons in the channel

$$q(x_o) = - \kappa_2\kappa_o \frac{\partial\phi_2}{\partial y} \qquad (9)$$

This criterion may seem a little arbitrary, however it is borne out in practice since the pinch off point as defined by (8) coincides with the electrostatic neutral point on the oxide surface, which is what one might expect in the practical device.

II.4 <u>The Iterative Solution</u>

The problem has been reduced to that of solving the potential equations in two regions; in the oxide

$$\nabla^2\phi_2 = 0 \qquad (10)$$

and in the semiconductor

$$\nabla^2\phi_1 = \frac{e}{\kappa_1\kappa_o}\left\{N_A - n_i \exp \beta(\phi_p - \phi_1)\right\} \qquad (11)$$

The conditions at the boundaries of both regions are of a simple type except at the common boundary of the two regions, (equations (7), (8), (9). However, these may be satisfied iteratively in the following manner.

Choose a trial pinch off point $P^{(o)}$, a trial current $J^{(o)}$, and a trial potential distribution $V^{(o)}(x)$ where $S < x < P^{(o)}$. Then the boundary conditions of both regions are of a simple type, since the

complicated boundary conditions have been replaced by a simple Dirichlet condition, and as we shall see the equations (10) and (11) may be solved directly by the analogue method yielding the potential distributions ϕ_1 and ϕ_2 in the respective regions. The resulting surface charge distribution $q^{(o)}(x)$ may be found from (7)

$$q^{(o)}(x) = \kappa_o(\kappa_2\underline{\nabla}\phi_2 - \kappa_1\underline{\nabla}\phi_1).\underline{n}$$

and thus a channel current $J^{(o)}(x)$ defined

$$J^{(o)}(x) = + \mu_n q^{(o)}(x) \frac{\partial V_o}{\partial x} \qquad (13)$$

A new trial current $J^{(1)}$ is defined by

$$J^{(1)} = \frac{1}{SP} \int_S^P J^{(o)}(x)dx$$

and a new surface potential distribution along the channel $V^{(1)}(x)$ may be found by integration of (7iii).

$$V^{(1)}(x) = - \frac{J^{(1)}}{\mu_n} \int_s^x \frac{dx}{q^{(o)}(x)} \qquad (x < P) \qquad (14)$$

In general $q^{(o)}(x)\Big|_{x=P} \neq 0$ and the end point of the channel may be adjusted accordingly. The procedure is repeated until convergence results. While no theoretical proof for the convergence from a particular trial solution, or of the uniqueness of the final solution can be offered, in practice it was found that the different trial solutions, under otherwise identical conditions led to the same final solution.

II.5 Trial Solution

It is essential to have good trial potential functions and current values etc., if the number of iterations are to be kept small. To this end the following simple theory was used.[5]
For a thin oxide layer:

$$\underline{\nabla}\phi_2.\underline{n} \simeq \frac{V_g - V(x)}{L} \qquad (15)$$

and for a narrow channel

$$\kappa_2\kappa_0 \, \underline{\nabla\phi_2}.\underline{n} \simeq - q(x) \qquad (16)$$

will hold so long as the field on the semiconductor side of the interface is small as compared to that in the oxide. If the channel current is constant then

$$J = q(x)\mu_n \frac{\partial V}{\partial x} \qquad (17)$$

Thus from (16), (17) and (18)

$$J = \frac{\mu_n \kappa_2 \kappa_0}{L} (V - V_g) \; \frac{dV}{dx} \qquad (18)$$

Integrating (18) gives

$$\frac{1}{2}V^2 - V\,V_g = \frac{JLx}{\mu_n \kappa_2 \kappa_0} \qquad (20)$$

Low Drain Voltages ($V_G > V_D$)

The trial current is determined from equation (20), using the condition that the potential at the end of the channel is V_D.

$$J = \frac{\mu_n \kappa_2 \kappa_0}{L.SD} \left[\frac{1}{2}V_D^2 - V_D V_G\right] \qquad (21)$$

The $V(x)$ which satisfies (20) is the trial potential distribution.

High Drain Voltages ($V_G < V_D$)

The pinch off point is determined by the condition $V \simeq V_g$, and $q(x)$ falls to zero at this point as is seen from (16). Equation (20) may be used to determine the trial current if the pinch off point is known. Thus

$$J = \frac{-\mu_n \kappa_2 \kappa_0}{2L.SP} V_g^2 \qquad (22)$$

The trial potential distribution follows immediately from (20).

It is apparent that no estimate of the pinch off point may be made on this model, since the approximations (15) and (16) used in deriving the expressions above become invalid at the pinch off point.

III - The Resistance Network Analogue

The approach to the problem, approximations and boundary conditions have been dealt with, in the previous section, on the basis of a continuous model. In this section the method of solution by a resistance network analogue is described. The design of the network is described only in outline since it involves well established techniques.

III.1 Design Considerations

The solution of the Shockley-Poisson equation by means of a resistance network has been described in last year's report. The analogue consists of a resistance network at whose nodes are injected two independent currents simulating respectively the impurity space charge and carrier space charge. The M.O.S.T. problem is simplified in that only the majority carriers need be represented in the bulk semiconductor, i.e.

$$\nabla^2\phi_1 = \frac{e}{\kappa_1\kappa_0}\left\{N_A - n_i \exp\beta\ \phi_\rho - \phi_1)\right\}$$

$$= \frac{eN_A}{\kappa_1\kappa_0}\left\{1 - \exp\beta\left[\phi_p + \frac{1}{\beta}\ln\frac{n_i}{N_A} - \phi_1\right]\right\}$$

and so the 'sinh term elements' and the current generators representing the impurity space charge may be replaced by simple diodes having characteristics of the form

$$i = i'_s\ (e^{\beta V} - 1).$$

The potential difference applied to the diodes in the R.N.W.A. is given by

$$V = \phi_\rho + \frac{1}{\beta}\ln\frac{n_i}{N_A} - \phi_1$$

where the nodes of the resistance network are at a potential ϕ_1, and $\phi_\rho + \frac{1}{\beta}\ln\frac{n_i}{N_A}$ is a constant potential.

A non-uniform rectangular array of points was chosen to represent the space of the device. The domain of the representative points is divided into cells by constructing normal bisectors between neighbouring points lying in the same principal plane.[6] Consider Poisson's equation;

$$\nabla^2\phi = -\rho$$

and integrating over the area of each cell then using Gauss's theorem

$$\underset{\text{cell}}{\iint} \nabla^2\phi \, d\tau = -\underset{\text{cell}}{\iint} \rho \, d\tau = \underset{\text{surface}}{\int} \underline{\nabla\phi} . \underline{ds}$$

A finite difference formula is constructed by summing the normal component of field over the surface of the cell, and by assuming that the charge of density ρ is uniform over the cell. Thus, using the notation indicated in the figure

$$\left\{\frac{\phi_1-\phi_o}{h_1} + \frac{\phi_2-\phi_o}{h_2}\right\}\frac{h_3+h_4}{2} + \left\{\frac{\phi_3-\phi_o}{h_3} + \frac{\phi_4-\phi_o}{h_4}\right\}\frac{h_1+h_2}{2} = -\rho_o\frac{1}{4}(h_1+h_2)(h_3+h_4)$$

Let a fundamental value of resistance R be chosen, then if

$$R_1 = \frac{2h_1R}{h_3+h_4} \; ; \qquad R_2 = \frac{2h_2R}{h_3+h_4}$$

$$R_3 = \frac{2h_3R}{h_1+h_2} \; ; \qquad R_4 = \frac{2h_4R}{h_1+h_2}$$

and

$$i'_s = \frac{(h_1+h_2)(h_3+h_4)eN_A}{4\kappa_-\kappa_o R}$$

then the finite difference equation corresponding to the Shockley-Poisson equation may be realised by a resistance network.

Similar principles are used in the choice of resistance values for nodes at or near the surface. These are of two types, those of fixed potential or those at which the normal component of field is specified.

The condition at the interface in the absence of surface charge are as follows:

$$\kappa_2 \frac{\partial \phi_2}{\partial y} = \kappa_1 \frac{\partial \phi_1}{\partial y}$$

or in terms of a finite difference equation

$$\frac{\kappa_1}{h_1}(\phi_o - \phi_1) = \frac{\kappa_2}{h_2}(\phi_2 - \phi_o)$$

If the terminating resistance values in the semiconductor and in the oxide are R_1 and R_2 respectively then if

$$R_2 = \frac{h_2 \kappa_1}{h_1 \kappa_2} R_1$$

the boundary conditions at the surface will be satisfied. R_1 will be fixed by conditions imposed one mesh spacing away from the surface and thus R_2 and the fundamental value of resistance in the oxide is also fixed.

In Figure 3 the network is shown and the values of resistance (in megohms) is indicated. Since the potential is more or less constant in the neutral region, the base contact has been shifted towards the gate, so as to economize on diode groups. In fact only about 200 matched diode groups were available which necessitated a coarser grid than would otherwise have been desirable. The grid is non-uniform rectangular being finer in the region of the channel than elsewhere.

IV Results

Measurements have been made of the drain/source characteristic for a gate voltage of 10 volts. The characteristic is shown in Figure (4). For several of the measured points the potential and charge variation along the channel is shown (Figure (5)). The potential distribution in the device is also shown for three representative drain voltages (Figures (6), (7) and (8)), and also the potential distribution is shown in the absence of a channel (Figure (9)). In Figure (10) is shown a diagram of the device showing the spatial distribution of mesh points; each mesh point is labelled with a potential (in volts) as measured for a drain voltage of 20 volts.

In Figure (11) the dependence of total electron charge stored in the channel upon drain voltage is shown.

A program for the Pegasus computer was written which used cubic interpolation of the charge distribution along the channel and deduced the trial potential function from the voltages along the mesh points of the channel and their neighbours. Although this was a success at drain voltages lower than the gate voltage, convergence was never achieved for drain voltage higher than the gate voltage. This was probably due to scatter in the measured points giving rise to error growth. However when the iteration procedure was carried through manually, drawing a 'best curve' through the measured value of q (x), convergence was achieved to 1% in the value of voltage at any mesh point in at the most six iterations.

Typically in the saturation region of an M.O.S.T. the drain characteristic displays a constant positive slope, proportional to the gate voltage. This has been attributed to the movement of pinch-off point towards the source electrode for drain voltages greater than the gate voltage. Given that the maximum electron concentration occurs at the source, then the maximum current would occur for a constant electron concentration over the length of the channel, falling abruptly to zero at the pinch off point, and an associated constant electric field V_G/SP over the length of the channel. The channel current would then be given by

$$J_{max} = - en(S) \frac{V_G}{SP}$$

This configuration can clearly never be achieved in practice however it is our contention that at high drain voltages the maximum current can be more nearly achieved than at lower drain voltages. Our results on the R.N.W.A. show that for drain voltages between 10 and 40 volts and a gate voltage of 10 volts there is a 19% decrease in channel length and a 43% increase in current, which would appear to substantiate our claim that the value of the slope resistance is not brought about solely by decrease in channel length.

A further feature which may be of interest which occurs in our results, once again as a consequence of the two-dimensional nature of the model, is the minimum of electron concentration, along the channel. This moves towards the drain voltage and disappears for quite a low drain voltage, however it would be of interest to determine its presence at a drain voltage of zero, when the electron fermi-level is constant throughout the base region. It is possibly worthy of note that the electron concentration at the source is independent of drain voltage.

The equi-potential diagrams provide a measure of quality of the approximation of neglect of transverse field in the integration of the potential distribution carried out in much of the theoretical work published. It is seen that although the approximation might be quite reasonable near the source at drain voltages lower than the gate voltage, near the drain the approximation becomes invalid, even at drain voltages lower than the gate voltage.

V. A Note on Errors

The truncation error in a partial difference scheme for Poisson's equation is well known and has been dealt with elsewhere. It is presumed that the error is not so large as to distort any feature of the potential distribution within the device and we shall not consider it further. What is of a more serious nature is the error involved in the treatment of the channel on a discrete model.

If diffusion is neglected and the channel is treated as a surface charge then the current

$$J = \mu_n q \frac{\partial V}{\partial x}$$

is presumed constant along the length of the channel. At the pinch off point P, $q(x) = 0$ and at a point $P-\epsilon$, $q(x) = -\epsilon q'(P)$ thus $\frac{\partial V}{\partial x} = -\frac{J}{\mu_n}\frac{1}{\epsilon q'(P)}$ and so long as $q'(P) \neq \infty$ then $\frac{\partial V}{\partial x} \rightarrow \infty$ at P, which is rather an undesirable consequence. Clearly it arises because of the form of the approximations which are made, for at the end of the channel the current does not abruptly terminate, but rather the carriers diffuse into the bulk

material. This singularity would be avoided if $J \to 0, x \to P$ but the distance Δx over which J tended from its constant value to zero must be such that $\left|\frac{\partial \phi}{\partial x}\Delta x\right| \sim \frac{kT}{e}$ in order that the model be consistent with behaviour in the device. Since in the analogue the mesh spacing along the interface is much greater than this, there is little point in making a correction of this order.

It is clear that the solution of the finite difference scheme for the channel will depend to some extent upon the choice of finite difference formulae. Also for physically meaningful solutions the maximum component of field along the channel is bounded

$$\left|\frac{\partial V_i}{\partial x}\right| \leq \frac{V_d - V_s}{h}$$

where h is the mesh spacing. Thus the problem of infinite field strength encountered in the continuous model cannot arise.

Acknowledgements

The work described in this report was carried out at the suggestion of Dr. F. Berz of Mullard Research Laboratories, Redhill, Surrey, and the authors are indebted to Dr. Berz and Mr. N. St. John Murphy for helpful discussion.

References

1. 'A Unipolar 'Field Effect' Transistor'. W. Shockley, Proc. IRE 40, 1365 1952.
2. 'The theory of p-n junctions in semiconductors and p-n junction transistors'. BSTJ 28, 441, 1949.
3. 'An Analogue Method for the Determination of Potential Distributions in Semiconductor Systems'. J.A. Davis, H.W. Loeb, CVD Project RU27-1, Annual Report, November, 1965.
4. 'Resistance Network Simulation of Semiconductor Systems'. H.W. Loeb, Proc. 4th International Analogue Computation Meeting, Brighton, 1964.

5. 'Physical Processes in Insulated-Gate Field Effect Transistors' J.E. Johnson. Solid State Electronics 7, 861, 1964.

6. 'Resistance Network Analogues with Unequal on Subdivided Meshes', G. Liebmann, B.J.A.P., 5, pp. 362-366 (1954).

Appendix A - The Surface Channel Approximation with Diffusion

This appendix parallels Sections II.4 and II.5 except that the effect of diffusion is included.

A1 - The Iterative Scheme

Choose $V^{(o)}(x)$, $J^{(o)}$, $P^{(o)}$ then, as before, there will be an associated $q^{(o)}(x)$ which may be measured on the analogue.

$$q^{(o)}(x) = \kappa_o(\kappa_2\underline{\nabla\phi_2} - \kappa_1\underline{\nabla\phi_1}).\underline{n} \qquad (1)$$

A current distribution $J^{(o)}(x)$ may be defined

$$J^{(o)}(x) = \mu_n\left\{q^{(o)}(x)\,\frac{dV^{(o)}(x)}{dx} - \frac{1}{\beta}\,\frac{dq^{(o)}(x)}{dx}\right\} \qquad (2)$$

and its average, $J^{(1)}$

$$J^{(1)} = \frac{1}{SP}\int_S^P J^{(o)}(x)dx$$

$$= \frac{\mu_n}{SP}\int_S^P q^{(o)}(x)\,\frac{dV^{(o)}(x)}{dx}\,dx + \frac{\mu_n}{\beta.SP}[q^{(o)}(S) - q^{(o)}(P)] \qquad (3)$$

A new potential distribution $V^{(1)}(x)$ consistent with $J^{(1)}$ and $q^{(o)}(x)$ is formed

$$J^{(1)} = \mu_n\{q^{(o)}(x)\,\frac{dV^{(1)}}{dx} - \frac{1}{\beta}\,\frac{dq^{(o)}}{dx}\}$$

whence

$$V^{(1)}(x) = \frac{J^{(1)}}{\mu_n}\int_o^x \frac{dx}{q^{(o)}(x)} + \frac{1}{\beta}\,\ell n\left\{\frac{q^{(o)}(x)}{q^{(o)}(S)}\right\} \qquad (4)$$

A new pinch off point $P^{(1)}$ may be defined by $q^{(o)}(x)\Big|_{x=P^{(1)}} = 0$ or by some other suitable criterion $J^{(1)}$, $V^{(1)}(x)$ are defined by (3) and (4) and thus the iterative procedure may be repeated.

A2 - The Trial Solution

The procedure is analagous to that in II.5 and we shall only quote the results.

Low drain voltages $V_D < V_G$

$$J = \frac{\mu_n \kappa \kappa_o}{2.L.SD}\left\{V_D^2 - 2V_D(V_G + \frac{1}{\beta})\right\} \tag{5}$$

$$\frac{x}{SD} = \frac{V^2(x) - 2V(x)(V_G + \frac{1}{\beta})}{V_D{}^2 - 2V_D(V_G + \frac{1}{\beta})} \tag{6}$$

High Drain Voltage $V_D > V_G$

As in II.5 it is impossible from such a theory to fix the pinch off point P. However, given this point

$$J = -\frac{\mu_n \kappa\kappa_o}{2.L.SP}\left\{V_G^2 + \frac{2}{\beta}V_G\right\} \tag{7}$$

$$\frac{x}{SP} = \frac{2V(V_G + \frac{2}{\beta}) - V^2}{V_G^2 + \frac{2}{\beta}V_G} \tag{8}$$

It is seen that diffusion is only a minor effect in the mode of operation which is being considered, since in this simple analysis a gate voltage of $V_G + \frac{1}{\beta}$ excluding the effect of diffusion, is equivalent to a gate voltage of V_G if diffusion is included.

Appendix B Solution with Approximation of Equations of Electron Fermi Level within the Base Region

The quasi-Fermi level for electrons is shown in Section II to satisfy the relationship

$$\nabla^2\phi_n + \beta(\underline{\nabla\phi}.\underline{\nabla\phi}_n - \underline{\nabla\phi}_n.\underline{\nabla\phi}_n) = 0 \qquad (1)$$

The boundary conditions at source and drain are respectively:

$$\phi_n(S) = V_S - \frac{1}{\beta}\ln\frac{N_D}{n_i}\,; \quad \phi_n(D) = V_D - \frac{1}{\beta}\ln\frac{N_D}{n_i} \qquad (2)$$

and elsewhere over the boundary of the base region the normal component of $\underline{\nabla\phi}_n$ is zero, in particular this is true at the oxide/semiconductor interface.

It is convenient at this stage to make the transformation

$$\phi_n = -\frac{1}{\beta}\ln z \qquad (3)$$

when (1) becomes

$$\nabla^2 z - \beta\,\underline{\nabla z}.\underline{\nabla\phi} = 0 \qquad (4)$$

For drain voltages lower than the gate voltage the channel extends from source to drain and to a good approximation the current flow is tangential to the oxide/semiconductor interface. The channel is narrow and thus the approximation that the electron Fermi-level is constant in the direction normal to the interface is probably reasonable. Thus (4) becomes

$$\frac{d^2z}{dx^2} - \beta\,\frac{dz}{dx}\,\frac{d\phi}{dx} = 0$$

and

$$\frac{dz}{dx} = Ae^{\beta\int_0^x \frac{d\phi}{dx}\,dx} = Ae^{\beta\phi(x)}$$

$$z = A\int_0^x e^{\beta\phi(x)}dx + B$$

where A and B are constants of integration. Applying the boundary

conditions (2) then

$$z(x) = \frac{N_D}{n_i}\left[e^{-\beta V_D} - 1\right] \frac{\int_S^x e^{\beta\phi} dx}{\int_S^D e^{\beta\phi} dx} + \frac{N_D}{n_i} \qquad (5)$$

whence

$$\phi_n(x) = -\frac{1}{\beta}\ln\frac{N_D}{n_i}\left[1 + [e^{-\beta V_D} - 1]\frac{\int_S^x e^{\beta\phi} dx}{\int_S^D e^{\beta\phi} dx}\right] \qquad (6)$$

and

$$n(x)\bigg|_{y=o} = e^{\beta\phi(x)}\left[\frac{N_D}{n_i}\left\{1 + [e^{-\beta V_D} - 1]\frac{\int_S^x e^{\beta\phi} dx}{\int_S^D e^{\beta\phi} dx}\right\}\right] \qquad (7)$$

If it is assumed that $\left|\frac{\partial^2\phi}{\partial x^2}\right| << \left|\frac{\partial^2\phi}{\partial y^2}\right|$ along the channel then the total electron density $n_t(x)$ may be found by integration.

$$\frac{\partial^2\phi}{\partial y^2} \simeq \frac{e}{\kappa\kappa_o}\left\{N_A - \rho + n_i e^{\beta(\phi-\phi_n)}\right\}$$

The approximation is made that both acceptor and hole concentrations are negligible in comparison with electron concentration near the oxide/semiconductor interface. Thus

$$\frac{\partial^2\phi}{\partial y^2} = \frac{en_i}{\kappa\kappa_o} e^{\beta(\phi-\phi_n)}$$

Integrating with respect to ϕ gives

$$\frac{1}{2}\left(\frac{\partial\phi}{\partial y}\right)^2 = \frac{en_i}{\kappa\kappa_o}\beta e^{\beta(\phi-\phi_n)} + c$$

where c is a constant of integration. Presuming boundary conditions $\frac{\partial\phi(o)}{\partial y}$ and $\phi(o)$ at the interface then

$$\frac{1}{2}\left(\frac{\partial\phi}{\partial y}\right)^2 = \frac{1}{2}\left(\frac{\partial\phi(o)}{\partial y}\right)^2 + \frac{en_i}{\beta\kappa\kappa_o} e^{-\beta\phi_n}\left[e^{\beta\phi} - e^{\beta\phi(o)}\right]$$

Now

$$n_i e^{\beta(\phi - \phi_n)} = n(x, y)$$

and

$$n_t(x) = \underset{y \to \infty}{\mathrm{Lt}} \int_0^y n(x,y)dy = \underset{y \to \infty}{\mathrm{Lt}} \left\{ \frac{\partial \phi}{\partial y} - \frac{\partial \phi(o)}{\partial y} \right\} \frac{\kappa \kappa_o}{e}$$

Thus

$$n_t(x) = \underset{y \to \infty}{\mathrm{Lt}} \frac{\kappa\kappa_o}{e} \left\{ \left[\left(\frac{\partial \phi(o)}{\partial y} \right)^2 + \frac{2en_i}{\beta\kappa\kappa_o} e^{-\beta\phi_n} \left(e^{\beta\phi} - e^{\beta\phi(o)} \right) \right]^{\frac{1}{2}} - \frac{\partial \phi(o)}{\partial y} \right\}$$

$$n_t(x) = \frac{\kappa\kappa_o}{e} \left\{ \left[\left(\frac{\partial \phi(o)}{\partial y} \right)^2 - \frac{2en(x,o)}{\beta\kappa\kappa_o} \right]^{\frac{1}{2}} - \frac{\partial \phi(o)}{\partial y} \right\}$$

This appendix shows that there exists an alternative procedure for iteration upon the resistance analogue, since from an initial potential distribution a surface charge distribution may be calculated, set up on the analogue, and the procedure repeated. The procedure is not equivalent to that used since the same assumption as to the electron charge distribution are not made.

Part B. A Numerical Method for the Solution of the Semiconductor Current Flow Equations

I. General

The solution of idealized models of semiconductor devices has undoubtedly contributed to progress both in design and in the evolution of new types of device from earlier times up to the present. Solutions of current flow and potential distributions provide insight into the workings of existing devices whilst at the same time giving guide lines in the design of future models. Theories of device operation, where they exist, frequently have limited ranges of application brought about by the approximations necessary to their derivation. In general the types of approximation in use are relatively few and well known, the aim of each is to produce a linear problem for which quite frequently analytic solutions exist. Typically these solutions could scarcely be bettered within the terms of the model by any other method and it is those problems which lie outside the scope of these analytic methods at which this work is aimed.

Our aim is to solve both time dependent and time independent situations. However the latter are viewed as asymptotic solutions of the time dependent equations. There are reasons for this approach; as far as we know no-one has solved the time independent current flow equations without approximation for any device model, however simple, without resort to approximation, even in one dimension where the equations become ordinary differential equations. It would seem that conventional methods of solving ordinary differential equations, numerically become highly unstable when applied to the semiconductor equations. The only method of solutions seems to be by the correction of a trial solution according to some algorithm, of which the method of finding the asymptotic solution of the time dependent equations may be viewed as a particular case.

In this report one particular finite difference representation of the time dependent equations is analysed and conditions are found for its stability and convergence in an approximate manner, the limitations

of the method are also discussed. As an example the carrier distribution within an abrupt symmetric p-n diode has been evaluated for the case of slight reverse bias.

At present the investigation is far from complete and extensions to the work will include the use of alternative finite difference representations; the extension to more than one spatial dimension; the speeding up of convergence when only the time independent solution is of importance, and the extension to a non-uniform rectangular grid of mesh points.

Following Gunn[1] (1958) we shall express the current and continuity equations for electrons and holes and Poisson's equation for potential distribution in normalized units. The normalized unit of length L and time τ are closely related to the Debye length and dielectric relaxation time of the intrinsic material, electron and hole concentrations n, p are normalized to the intrinsic concentration n_i, and the electrostatic potential ϕ is normalized to the mean thermal energy per degree of freedom $\frac{kT}{e}$. In terms of rationalized m.k.s. units the normalized units are given by

$$L = \left(\frac{kT\kappa\kappa_o}{e^2 n_i}\right)^{\frac{1}{2}}; \quad \tau = \frac{L^2}{D} \tag{1}$$

and the equations of semiconductor transport are

$$\underline{u}_n = + b(n\underline{\nabla\phi} - \underline{\nabla n}) \tag{2}$$

$$u_p = - p\underline{\nabla\phi} - \underline{\nabla p} \tag{3}$$

$$\frac{\partial n}{\partial t} = \pi_n - \underline{\nabla}.\underline{u}_n \tag{4}$$

$$\frac{\partial p}{\partial t} = \pi_p - \underline{\nabla}.\underline{u}_p \tag{5}$$

$$\nabla^2\phi = - p + n - \Omega \tag{6}$$

where $\underline{u}_n$, $\underline{u}_p$ are electron and hole fluxes; b is the ratio of electron to hole mobility; π_n, π_p are generation rates of electrons and holes

respectively by all processes (excluding drift), and Ω is tne net impurity density. These equations are derived on the presumption that the device may be represented by a system whose particles possess only an averaged behaviour, and thus it will not be expected that the solution of equation (2) - (6) will give any information with regard to noise.

A further simplification which has been made in the numerical solution of these equations is with respect to the impurity charge density Ω. In practical systems this is a time varying quantity since the charge on the traps and recombination centres fluctuate with carrier concentration, and if it is required to treat Ω as such then further conservation equations of the type (4) (5), may be written for the different charge states accounted for by the term Ω in Poisson's equation. However, for ease of computation, Ω has been treated as time-independent throughout.

II. The Finite Difference Scheme

If $\underline{u}_n$ is eliminated between (2) and (4) and $\underline{u}_p$ between (3) and (5) then

$$\frac{\partial n}{\partial t} = \pi_n + b\{\nabla^2_n - \underline{\nabla n}.\underline{\nabla \phi} - n\nabla^2\phi\} \qquad (7)$$

$$\frac{\partial p}{\partial t} = \pi_p + \nabla^2 p + \underline{\nabla p}.\underline{\nabla \phi} + p\nabla^2\phi \qquad (8)$$

(7) and (8) are 'diffusion' equations of parabolic type for the electron and hole density respectively, the equations are coupled by the electrostatic field ($\underline{E} = -\underline{\nabla\phi}$) and the space charge density ($\rho = -\nabla^2\phi$). The field is determined from (6).

$$\nabla^2\phi = -\rho = n - p - \Omega \qquad (6)$$

(7) and (8) are solved as initial value problems. This involves a choice of n and ρ at some initial time $t = t_o$. The equations (7) and (8) are solved by techniques and difference equations similar to those employed in the numerical solution of the heat diffusion equation. At $t = t_o$ and subsequently at every stage in the procedure the electrostatic field may be calculated by solution of (6). Thus (7) and (8) may be regarded as having time and spatially dependent coefficients, $E(x,t)$ and $\rho(x,t)$, and

may be treated otherwise as though they were linear. It is clear that a total of six boundary conditions are necessary for the solution of (6), (7) and (8), i.e. two for each equation. In the simplest case all three equations present boundary value problems but there are a large number of other possibilities upon which we shall not elaborate.

A finite difference scheme is set up by choosing a grid of points spanning the domain of x for which solutions are sought. Let there be N of these points labelled 1 .... N, separated by a constant difference Δx. A constant step length in time Δt is chosen and the differentials occurring in (6), (7) and (8) are replaced by their lowest order finite difference equivalents, thus, after some rearrangement

$$n_i^{j+1} = n_i^j + \Delta t(\pi_n)_i^j + b\frac{\Delta t}{(\Delta x)^2}\left\{n_{i+1}^j\left[1 + \frac{E_i^j \Delta x}{2}\right] + n_i^j\left[\rho_i^j(\Delta x)^2 - 2\right] + n_{i-1}^j\left[1 - \frac{E_i^j \Delta x}{2}\right]\right\} \tag{9}$$

$$p_i^{j+1} = p_i^j + \Delta t(\pi_p)_i^j + \frac{\Delta t}{(\Delta x)^2}\left\{p_{i+1}^j\left[1 - \frac{E_i^j \Delta x}{2}\right] - p_i^j\left[\rho_i^j(\Delta x)^2 + 2\right] + p_{i-1}^j\left[1 + \frac{E_i^j \Delta x}{2}\right]\right\} \tag{10}$$

$$\phi_{i+1}^j - 2\phi_i^j + \phi_{i-1}^j = (\Delta x)^2(n_i^j - p_i^j - \Omega_i^j) = -(\Delta x)^2 \rho_i^j \tag{11}$$

where

$$E_i^j = -\frac{1}{2\Delta x}\left[\phi_{i+1}^j - \phi_{i-1}^j\right]$$

In the equations above the superscripts denote the time variable and the subscripts the spatial variable. Having chosen p_i^1, n_i^1 for $(i = 1 \;....\; N)$, (11) may be evaluated yielding ϕ_i, $(i = 1 \;....\; N)$ then p_i^2, n_i^2 may be evaluated from (9) and (10), when the cycle is complete and the procedure may be repeated. The particular finite difference representation chosen is not unique, however it is possibly the most simple and has the decided advantage of being explicit. Other difference representations will be considered in due course.

III. Stability and Convergence

To find the conditions under which the 'exact' solution of the difference equations approximates to the solution of the partial differential equation, under the same conditions, is the problem of convergence. To find the conditions under which the numerical solution of the difference equations approximates to the exact solution of the difference equations is the problem of stability. (The difference between the exact and numerical solution of the difference equation is normally due to round off error). Both stability and convergence will depend upon several factors, in particular these will include, boundary and initial conditions and step lengths Δx and Δt, and in a successful solution of the problem Δx and Δt must be chosen, if possible, so as to achieve stability and convergence everywhere.

Because of the non-linearity of the difference equations, the derivation of conditions upon the variable quantities mentioned above, in order that stability and convergence do ensue, is probably impossible. However, the realization that the physical system represented is almost certainly well conditioned and that the difference equations provide a close analogy to the way in which changes of state in the physical system are brought about, relieve the difficulty, and it is found that physically realistic trial distributions and boundary conditions are well-conditioned in a mathematical sense. However this does not help in the choice of step lengths.

The criterion which fixes Δx is normally related to accuracy. Mesh points must be sufficiently close together so that the finite difference approximation to any particular differential involves little error. If only the asumptotic solution is of interest then a knowledge of the bounds of all the associated functions (e.g. $p, \frac{dp}{dx}, \frac{d^2p}{dx^2}, E, \frac{dE}{dx}, \ldots$) in the asymptotic state will allow a reasonable choice of Δx, but if details of the time dependent solution is required then a knowledge of these parameters at all stages in the procedure becomes important. Usually the information in either case will not be available and a reasonable guess of the minimum

step length must be substituted. For speed of calculation Δx must be kept as large as possible since the computing time required rises approximately as $(\Delta x)^{-3}$.

The best method of choosing a value of Δt is by the Fourier method of error analysis for linear difference equations. This is achieved by linearizing the diffusion equations (9) and (10) by choosing that the field and space charge density are constants over the domain in which analysis is made. Thus the conditions for stability are really conditions for a 'local stability'. It is typically found that for the mesh size which is used in practical calculations that the approximation of constancy of p and E is not really valid, however the results of this analysis are so useful in practice that the method is justified.

(9) and (10) have the same form as

$$\phi_i^{j+1} = \phi_i^j + s\left[(1-\gamma)\phi_{i+1}^j - (2+\xi)\phi_i^j + (1+\gamma)\phi_{i-1}^j\right] \quad (12)$$

if we linearise the recombination term and include its effect in the ξ of (12). We shall analyse the stability of this equation by the Fourier method and draw some conclusions as to the stability and convergence of (9), (10) and (11).

IV. The Error Analysis

Because of the linearity of (12) an error will propagate according to this same difference scheme. At $t = 0$ Fourier analysis may be made of the error in the row of N mesh points (we shall label the error as ψ)

$$\psi_i = \sum_n A_n e^{i\alpha_n x_i} \quad (13)$$

The error will propagate according to the difference equation (12) and it may be shown that if no further errors are introduced for $t > 0$ then the error at time t is given by

$$\psi_i = \sum_n A_n e^{\beta_n(\alpha_n)t} e^{i\alpha_n x_i} \quad (14)$$

It is sufficient to consider the behaviour of the component of (14), $e^{\beta t}e^{i\alpha x}$. Substituting this into (12)

$$e^{\beta\Delta t} = 1 + s\left\{(1-\gamma)e^{i\alpha\Delta x} - (2+\xi) + (1+\gamma)e^{-i\alpha\Delta x}\right\} \quad (15)$$

The von Neumann condition for stability is that

$$\left|e^{\beta\Delta t}\right| \leq 1 \quad (16)$$

and

$$\left|e^{\beta\Delta t}\right|^2 = \left[1+s\{2\cos\alpha\Delta x - (\xi+2)\}\right]^2 + 4s^2\gamma^2\sin^2\alpha\Delta x \quad (17)$$

In (16) the frequencies α were not discussed, we shall now consider that α is a continuous variable and thus satisfy (16) in the most restrictive case.

$$\frac{\partial\left|e^{\beta\Delta t}\right|^2}{\partial(2\Delta x)} = 4s\sin\alpha\Delta x\left[1-s(\xi+2) + 2s(1+\gamma^2)\cos\alpha\Delta x\right]$$

$$= 0 \text{ if } \begin{cases} \alpha\Delta x = n\pi, \ (n=0, \pm 1, \pm 2 \ \ldots.) \\ \cos\alpha\Delta x = \dfrac{1-s(\xi+2)}{2s(1+\gamma^2)} \end{cases}$$

Having found the conditions for the extrema of (17), the von Neumann condition may be applied at these points.

Case I - $\sin\alpha\Delta x = 0$ thus $\cos\alpha\Delta x = \pm 1$

$\cos\alpha\Delta x = +1$

$$\left|e^{\beta\Delta t}\right|^2 = (1-s\xi)^2$$

and

$$\left|e^{\beta\alpha t}\right|^2 \leq 1 \text{ if } \begin{cases} \xi > 0, \ 0 \leq s \leq \frac{2}{\xi} \\ \xi = 0, \ -\infty \leq s \leq +\infty \\ \xi < 0, \ \frac{2}{\xi} \leq s \leq 0 \end{cases} \quad (18)$$

$\cos\alpha\Delta x = -1$

$$\left|e^{\beta\Delta t}\right|^2 = [1-s(\xi+4)]^2$$

and
$$\left|e^{\beta\Delta t}\right|^2 \leq 1 \text{ if } \begin{cases} \xi > -4, \ 0 \leq s \leq \frac{2}{4+\xi} \\ \xi = -4, \ -\infty \leq s \leq +\infty \\ \xi < -4, \ \frac{2}{4+\xi} \leq s \leq 0 \end{cases} \quad (19)$$

Case II - $\cos \alpha\Delta x = \frac{1-s(\xi+2)}{2s(1+\gamma^2)}$

$$\left|e^{\beta\Delta t}\right|^2 = 4s^2\gamma^2 + \frac{\gamma^2(\gamma^2-1)(1-s(\xi+2))^2}{(1+\gamma^2)^2} \quad (20)$$

The condition that $\left|e^{\beta\Delta t}\right|^2 \leq 1$ is more complicated in this case since the limits of the range of s depend upon both ξ and γ. However for $\xi = 0$ the conditions become

$$\left|e^{\beta\Delta t}\right| \leq 1 \text{ if } -\frac{1}{2\gamma^2} \leq s \leq \frac{3\gamma^2+1}{2\gamma^2(3+\gamma^2)} \quad (21)$$

For $\xi \neq 0$ the conditions for stability may be written as

$$S_-(\xi,\gamma) \leq s \leq S_+(\xi,\gamma) \quad (22)$$

in which $S_\pm(\xi,\gamma)$ may be obtained from (20). In Figure (3) $S_\pm(0,\gamma)$ and $S_\pm(\pm 1,\gamma)$ are shown. It is seen that the limitations upon s in order that stability might occur for large γ is little affected by the actual value of ξ (at least for $|\xi| < 1$, a condition which will normally hold in practice). Because of this independent tendency for the conditions of stability as defined by Case I and Case II above, it will be convenient to distinguish instability as being of ξ or γ-type. Figure (2) shows the region of ξ stability and figure (3) the region of γ stability. In all solutions the steplength ratio s must be chosen such that the difference equation is both γ and ξ - stable.

It is seen that there is no region of ξ-stabilty for any value of s for $-4 \leq \xi \leq 0$ and that for $\xi \leq -4$ the region of stability corresponds to $s < 0$. This result for $\xi < 0$ is unfortunate, however, it is believed that inherent in the difference equations are other types of stability caused by the coupling of electron and hole flow. This we have not yet been able to analyse, however it is felt that the results of this analysis does not represent the whole truth for $\xi < 0$. Confirmation of this is provided by some recent

results (not given here) in which recombination/generation effects were excluded. In this case, according to the results of the above analysis, instability must occur in either the hole equation or electron according to the sign of the space charge. However for $s < \frac{1}{2}$ there were none of the usual signs of instability, and it seems likely that stability in either the electron or hole equation (in terms of the results of this analysis) is a sufficient condition for overall stability, though more work is required to test this hypothesis. Having proved the circumstances under which stability occurs, it follows that convergence occurs under the same conditions. (Lax's theorem). John (1952) and Richtmeyer (1957) have considered the same linear difference equation but have been concerned only with stability and convergence under the assumption that $\gamma, \xi \rightarrow 0$ whilst s remains finite. Currently we are trying to find the conditions for convergence of the linearized equation (12) by the matrix method in the range $-4 \leq \xi \leq 0$, but this work is incomplete.

The Abrupt p-n Junction

The carrier profiles within an abrupt p-n junction are shown in Figure (1B). These results are obtained as an asymptotic solution of the time dependent equations. The mesh size $\Delta x = 2 \times 10^{-2}$, $\Delta t = 1.5 \times 10^{-4}$ was chosen giving a mesh ratio $\frac{\Delta t}{(\Delta x)^2}$ of 0.375. The doping on either side of the junction is symmetric with $|\Omega| = 10^{-3}$. Generation/recombination effects are provided by a recombination centre which was chosen as being centre of the band and having equal trapping constants α for holes and electrons. Thus

$$\pi_n = \pi_p = \frac{\alpha n_t (np - 1)}{n + p + 2}$$

where n_t is the trap density, assumed uniform over the domain. The choice was made $\alpha = 10$, $n_t = 10$ giving a minority lifetime in the bulk of 10^{-2} and an associated minority carrier diffusion length 10^{-1}. The charge on the recombination centres is neglected in Poisson's equation.

The boundary conditions were chosen as follows:-

$$\phi_N = 11.8155, \ \phi_1 = 0$$

$$n_1\rho_1 = n_N\rho_N = 1$$

$$\rho_1 = \rho_N = 0$$

where the subscripts 1, N refer to p and n-type boundaries. The trial solution was given by

$$n_i p_i = 2; \ n_i - p_i - \Omega_i = 0 \qquad (i = 2, \ldots, N-1)$$

The number of mesh points spanning the x domain was 100, and 1,000 iterations were performed to achieve the results shown in figure 1B. After this time the maximum proportional rate of change of carrier concentration per interval of time $\Delta t, (\frac{\Delta \ell n \rho}{\Delta t})$, was less than 0.01%. The ratio b of electron to hole mobility is unity and thus the profiles possess the symmetry $n(x) = p(-x)$.

This model was chosen for speed and convergence and clearly does not attempt to simulate a practical device, as is seen where the dimensionless units are converted into practical units using data for silicon. The results obtained also gave complete information regarding current distribution, generation rate, electric field and potential distribution. We have omitted to give these here because of certain inaccuracies in the computed solution all of which may easily be remedied. The inaccuracies are due to:-

(a) The step length Δx is too large to give an accurate finite difference representation in the space charge region.

(b) Poisson's equation was solved using a double integration by the trapezoidal rule. This was inaccurate in the region of the junction.

For these reasons it is best not to draw any physical conclusions from the solution, which was included only to demonstrate the feasibility of solving junction problems.

VI. Summary

A method has been described for the solution of one-dimensional time varying semiconductor current flow problems and results have been presented in a simple case. Approximate conditions for stability of solution have been discussed. Below we summarize the conditions under which solution may be difficult under existing circumstances. Two types of difficulty are expected. The first is the absence, in a particular problem of either stability on convergence. The second is more trivial, the amount of computer time required may render the solution impractical. A way of alleviating this second difficulty is by the use of a non-uniform rectangular mesh with respect to its spacing both in x and t directions. The number of mesh points necessary is immediately reduced and it is likely that the average step length in time Δt may be increased, hence reducing the amount of computation. The first difficulty may probably be removed by the use of alternative difference formula, though it is likely that all problems may be solved by the use of sufficiently small step lengths.

References

1. Gunn, J.B. Journal of Electronics and Control IV, 1, (1958).

2. John.F. Commun. Pure Appl. Math. 5, 155-211 (1952).

3. Richtmeyer, R.D. 'Difference Methods for Initial Value Problems' London - Interscience (1957).

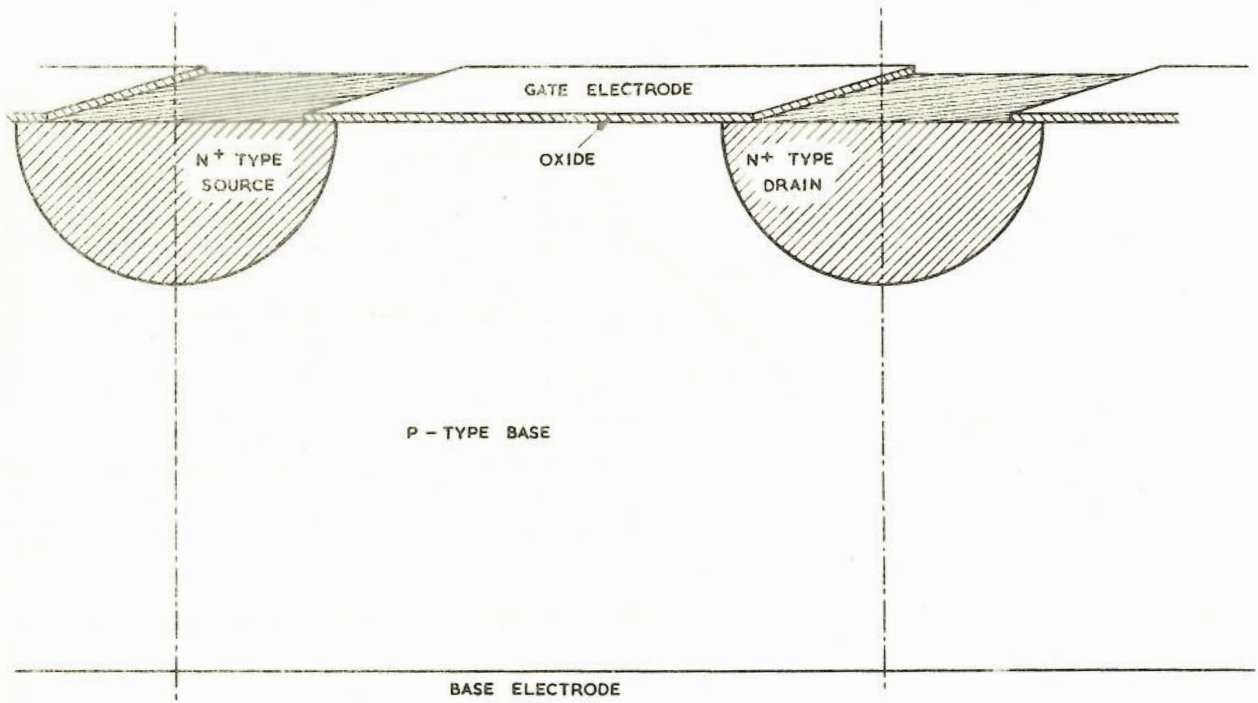

SCALE $\rightarrow\!|1\mu|\!\leftarrow$

WIDTH OF WAFER (NOT TO SCALE) $= 100\mu$

WIDTH OF OXIDE $= 0{\cdot}2\mu$

FIG. 1 THE PRACTICAL M.O.S.T DEVICE

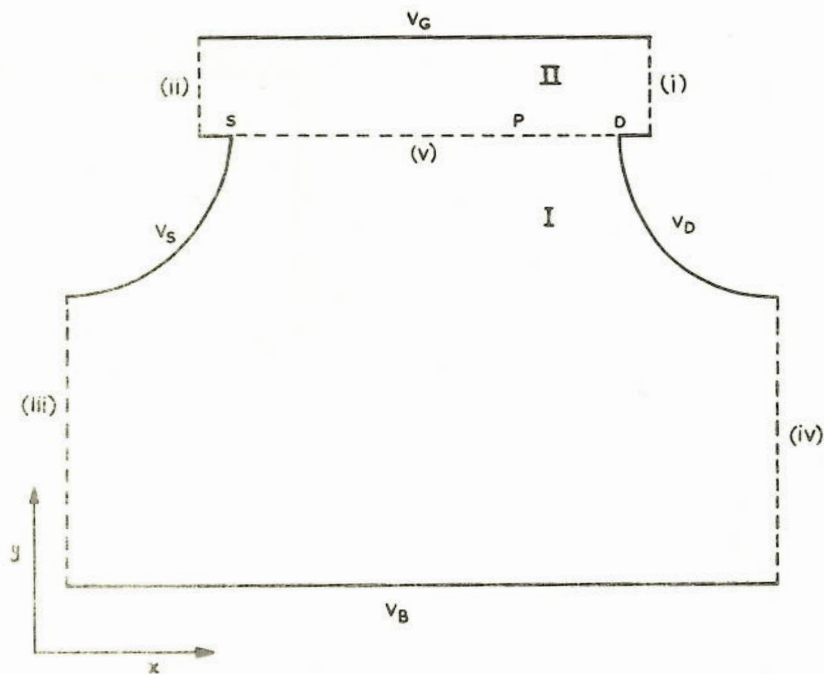

FIG. 2 M.O.S.T (DIAGRAMMATIC)

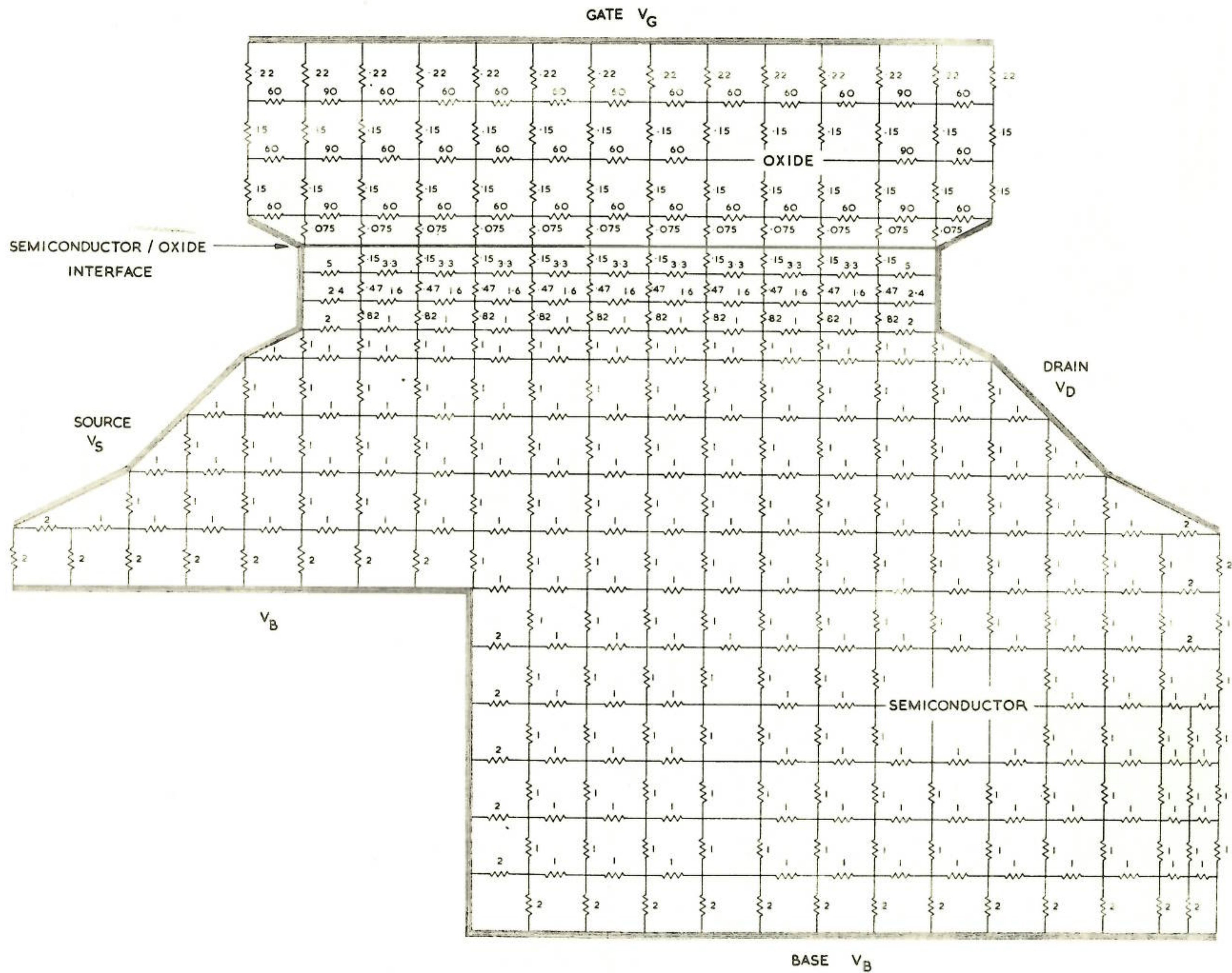

FIG. 3 THE RESISTANCE NETWORK

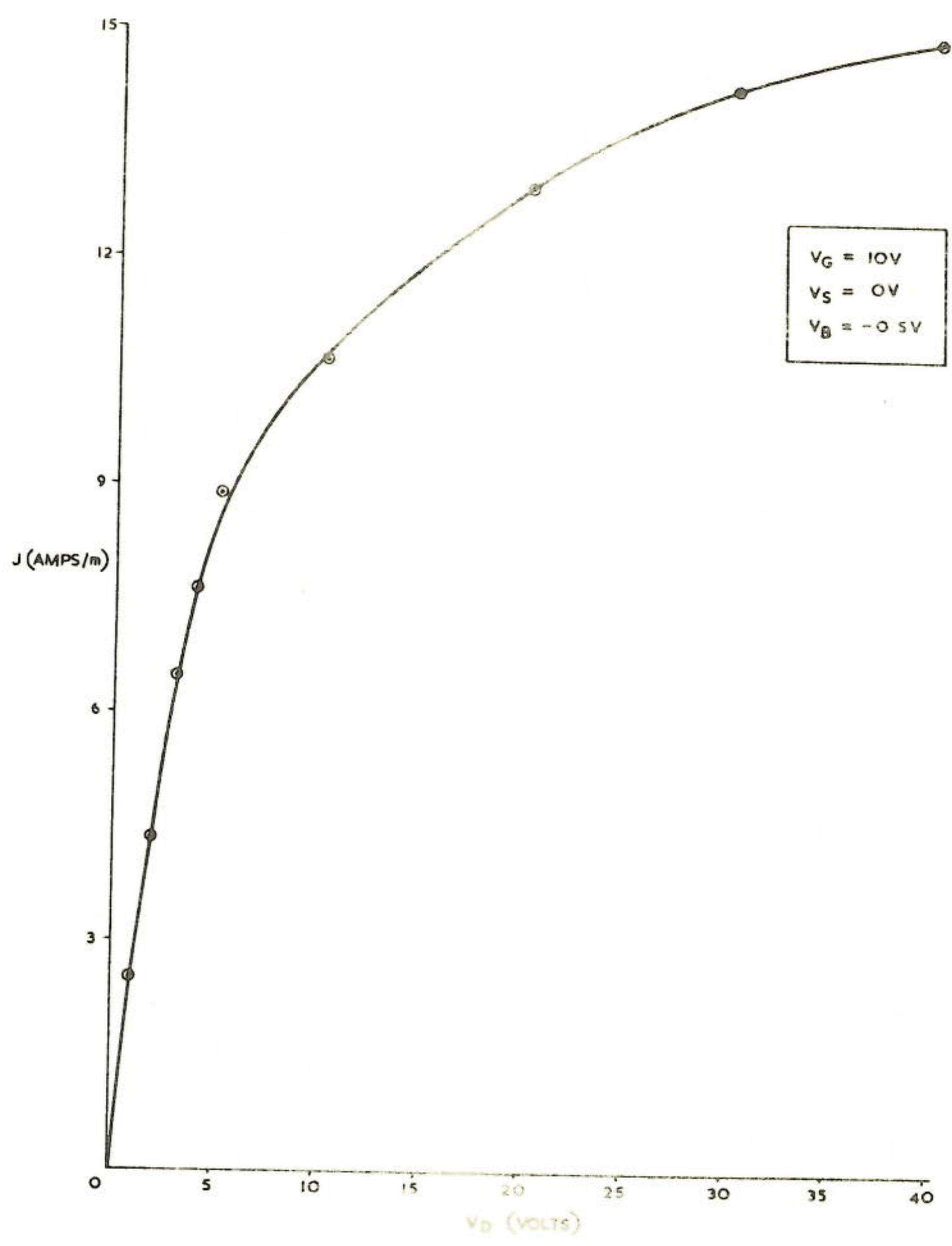

FIG. 4 CURRENT - VOLTAGE CHARACTERISTIC

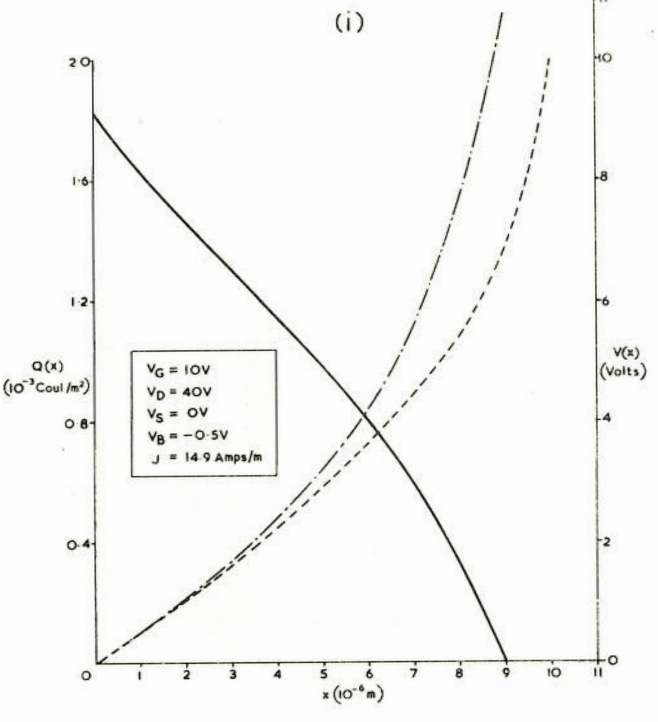

(i)
Q(x)
(10^{-3} Coul/m^2)
V(x)
(Volts)
V_G = 10V
V_D = 40V
V_S = 0V
V_B = −0·5V
J = 14·9 Amps/m
x (10^{-6} m)

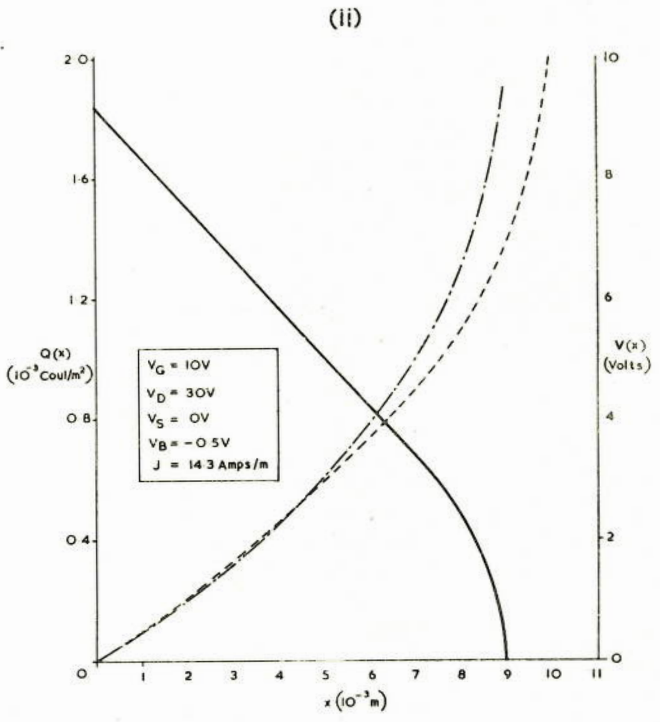

(ii)
Q(x)
(10^{-3} Coul/m^2)
V(x)
(Volts)
V_G = 10V
V_D = 30V
V_S = 0V
V_B = −0·5V
J = 14·3 Amps/m
x (10^{-3} m)

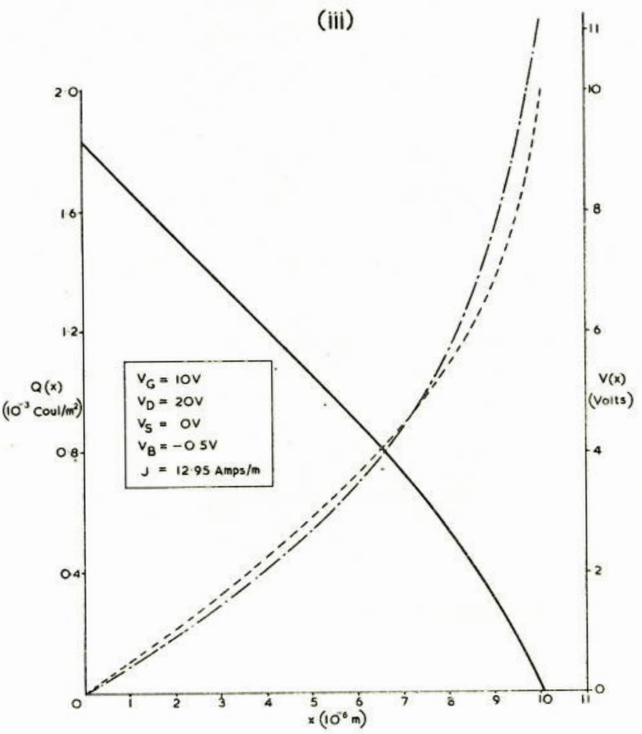

(iii)
Q(x)
(10^{-3} Coul/m^2)
V(x)
(Volts)
V_G = 10V
V_D = 20V
V_S = 0V
V_B = −0·5V
J = 12·95 Amps/m
x (10^{-6} m)

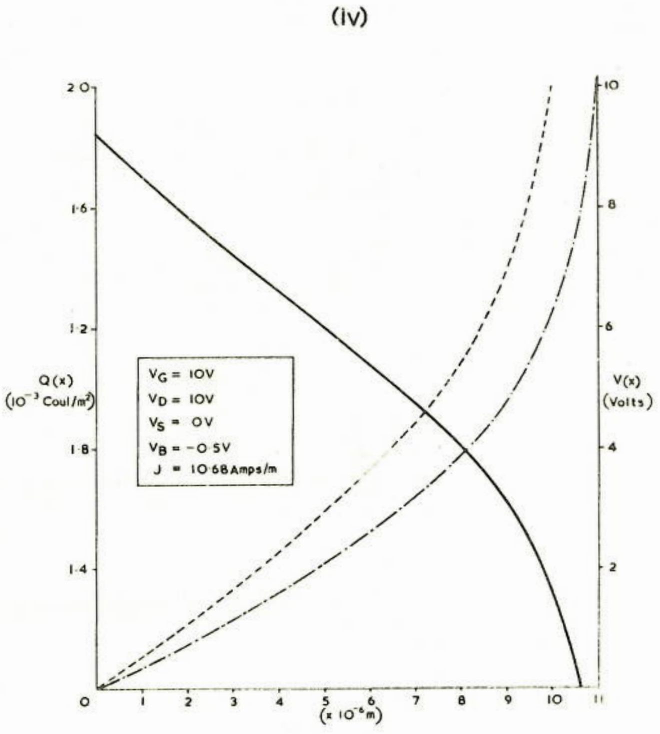

(iv)
Q(x)
(10^{-3} Coul/m^2)
V(x)
(Volts)
V_G = 10V
V_D = 10V
V_S = 0V
V_B = −0·5V
J = 10·68 Amps/m
(x 10^{-6} m)

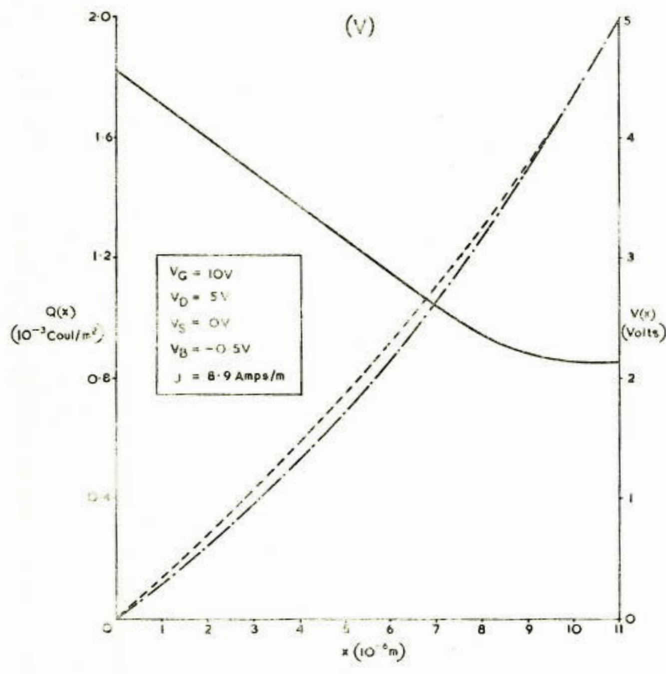

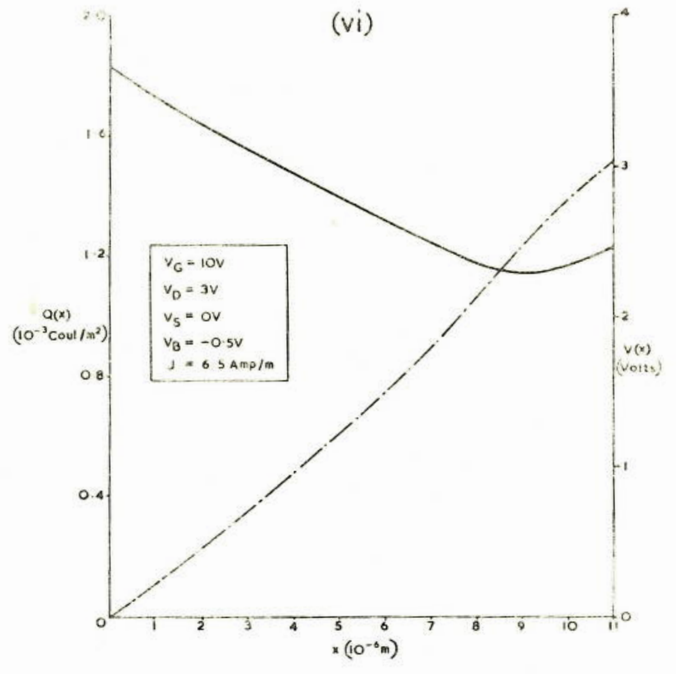

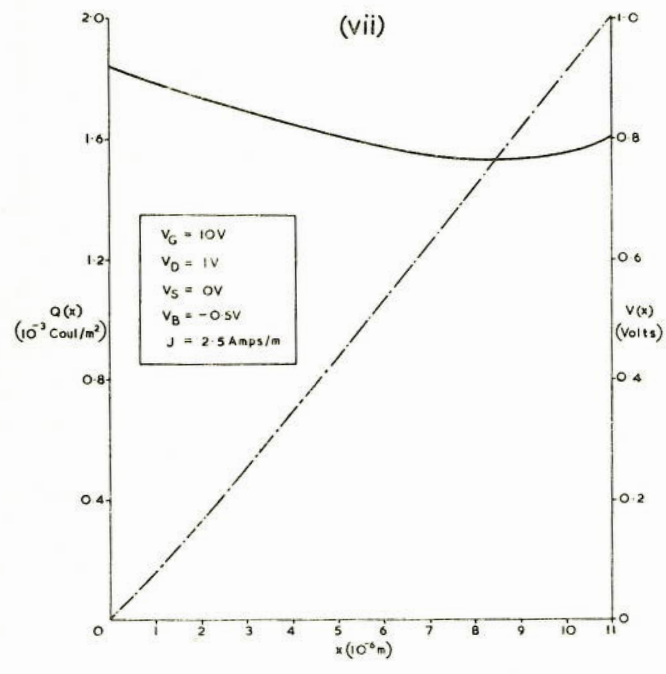

——— Q(x)
- - - - - $V^{(0)}(x)$
—·—·— V(x)

POTENTIAL AND CHARGE DISTRIBUTION ALONG OXIDE / SEMICONDUCTOR INTERFACE SHOWING TRIAL POTENTIAL $V^{(0)}(x)$

FIG. 5

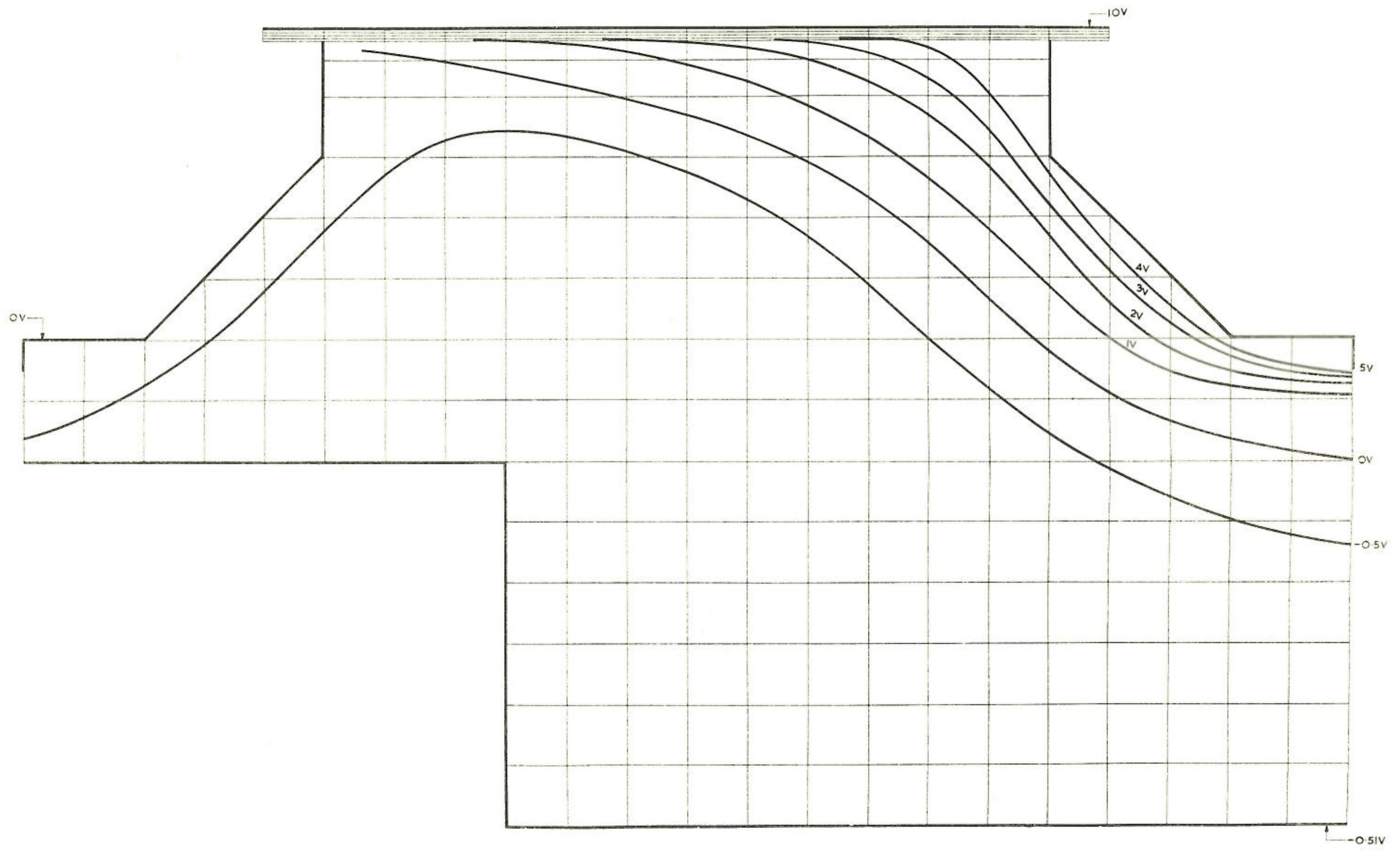

FIG. 6 POTENTIAL DISTRIBUTION IN M.O.S.T WITH DRAIN VOLTAGE OF 5 VOLTS

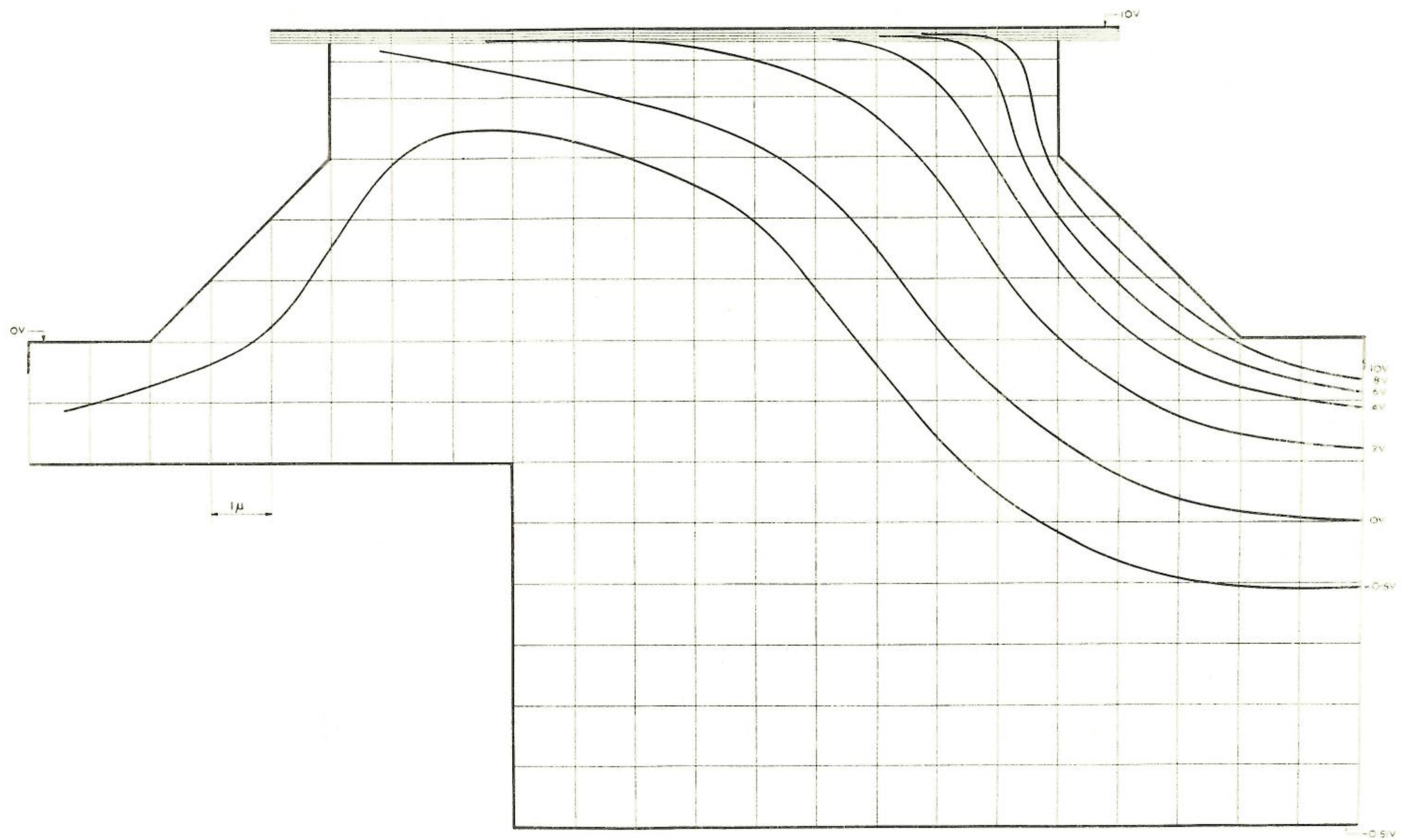

FIG. 7 POTENTIAL DISTRIBUTION IN M.O.S.T WITH DRAIN VOLTAGE OF 10 VOLTS

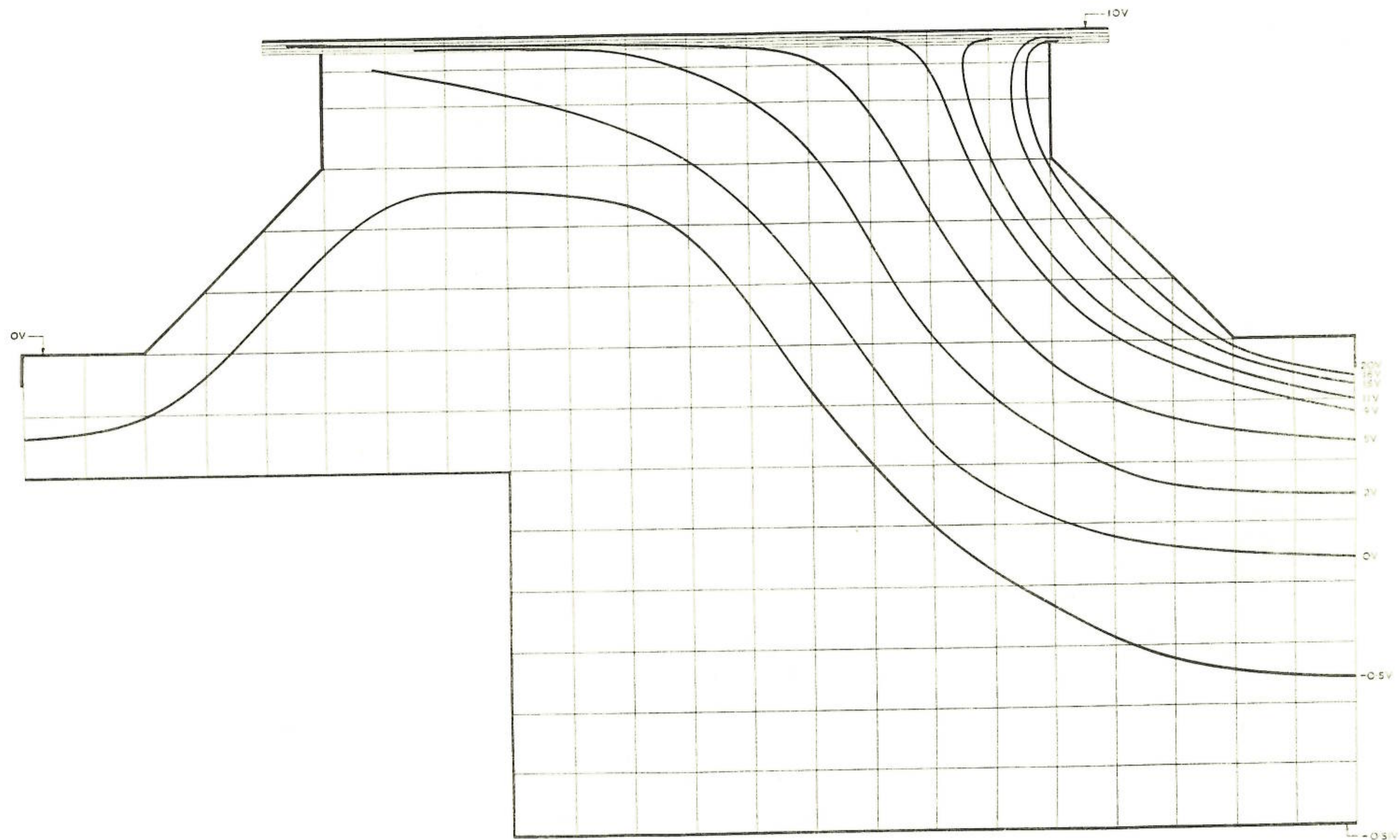

FIG 8 POTENTIAL DISTRIBUTION IN M O S T WITH DRAIN VOLTAGE OF 20 VOLTS

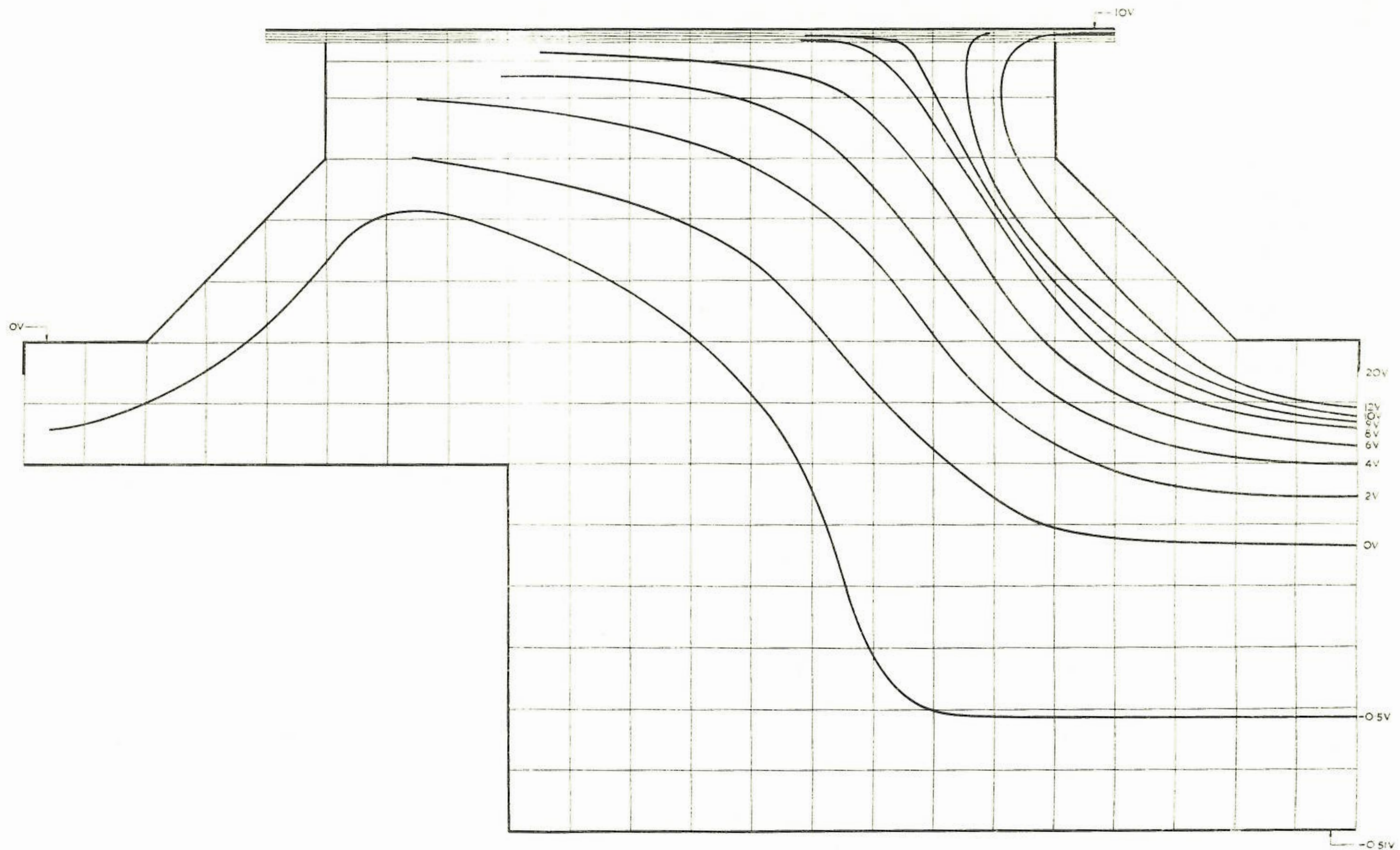

FIG. 9 POTENTIAL DISTRIBUTION IN M.O.S.T. WITH DRAIN VOLTAGE OF 20 VOLTS IN THE ABSENCE OF A CHANNEL

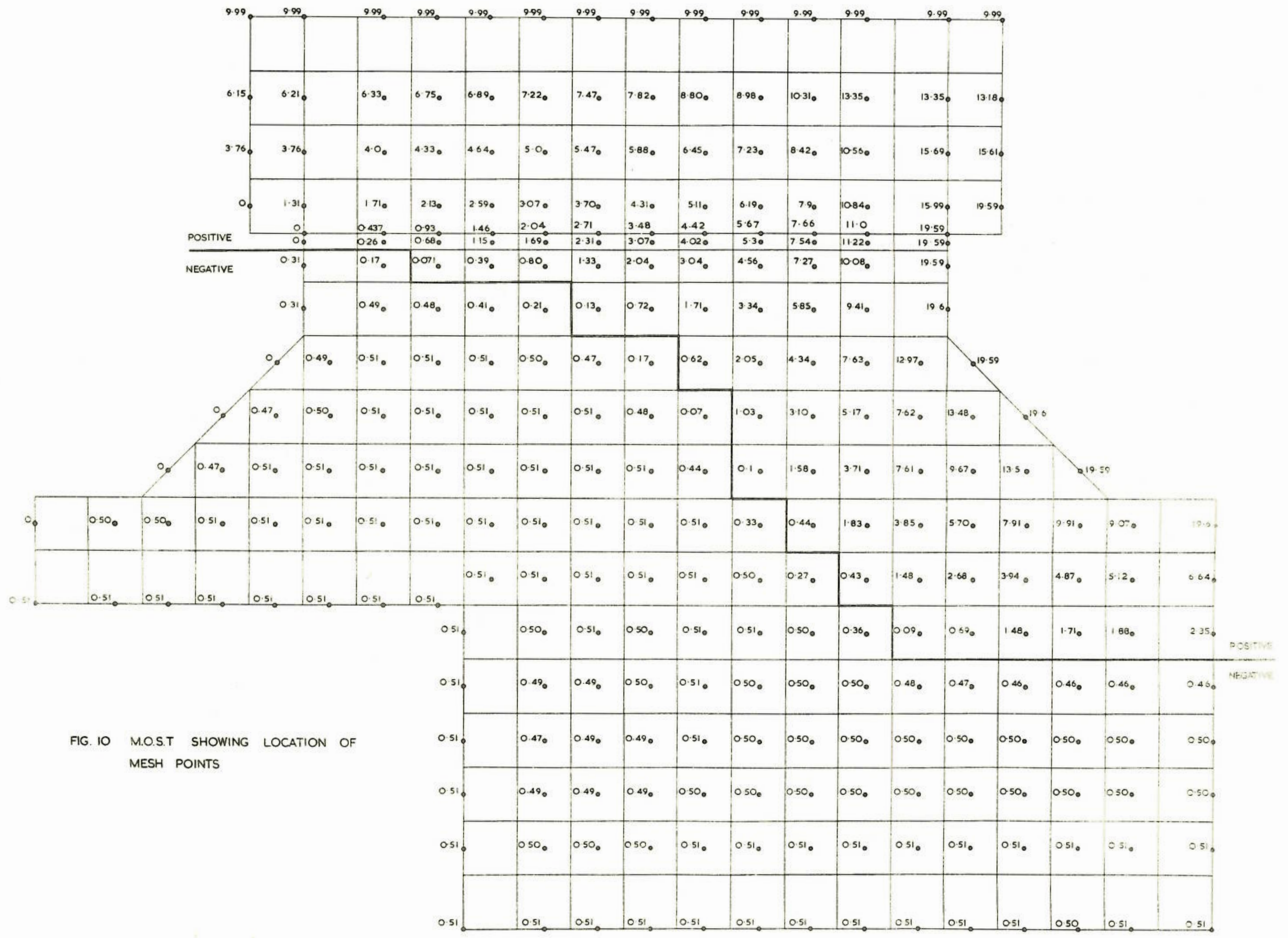

FIG. 10 M.O.S.T SHOWING LOCATION OF MESH POINTS

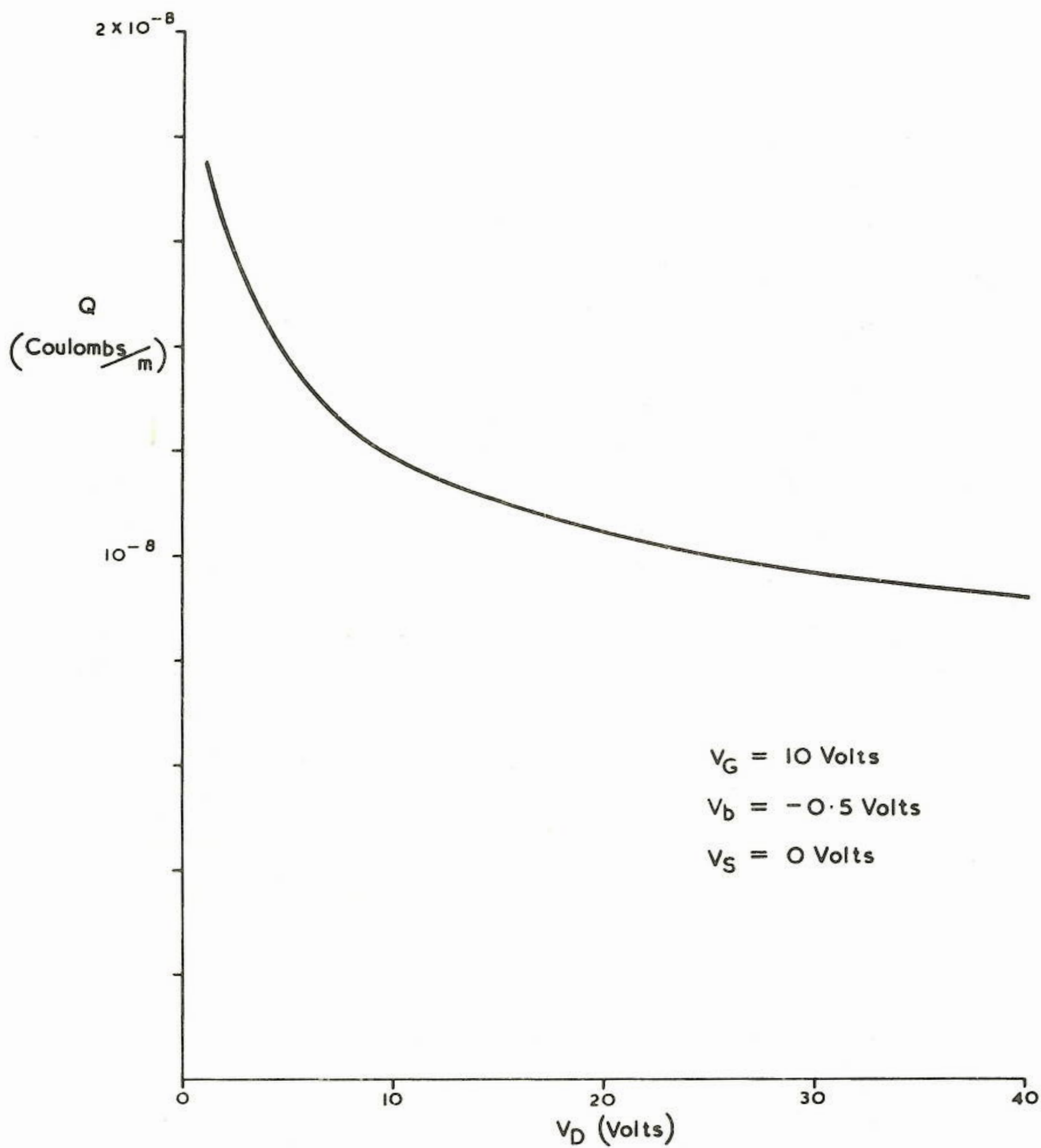

FIG. 11 TOTAL ELECTRON CHARGE IN CHANNEL AS A FUNCTION OF DRAIN VOLTAGE

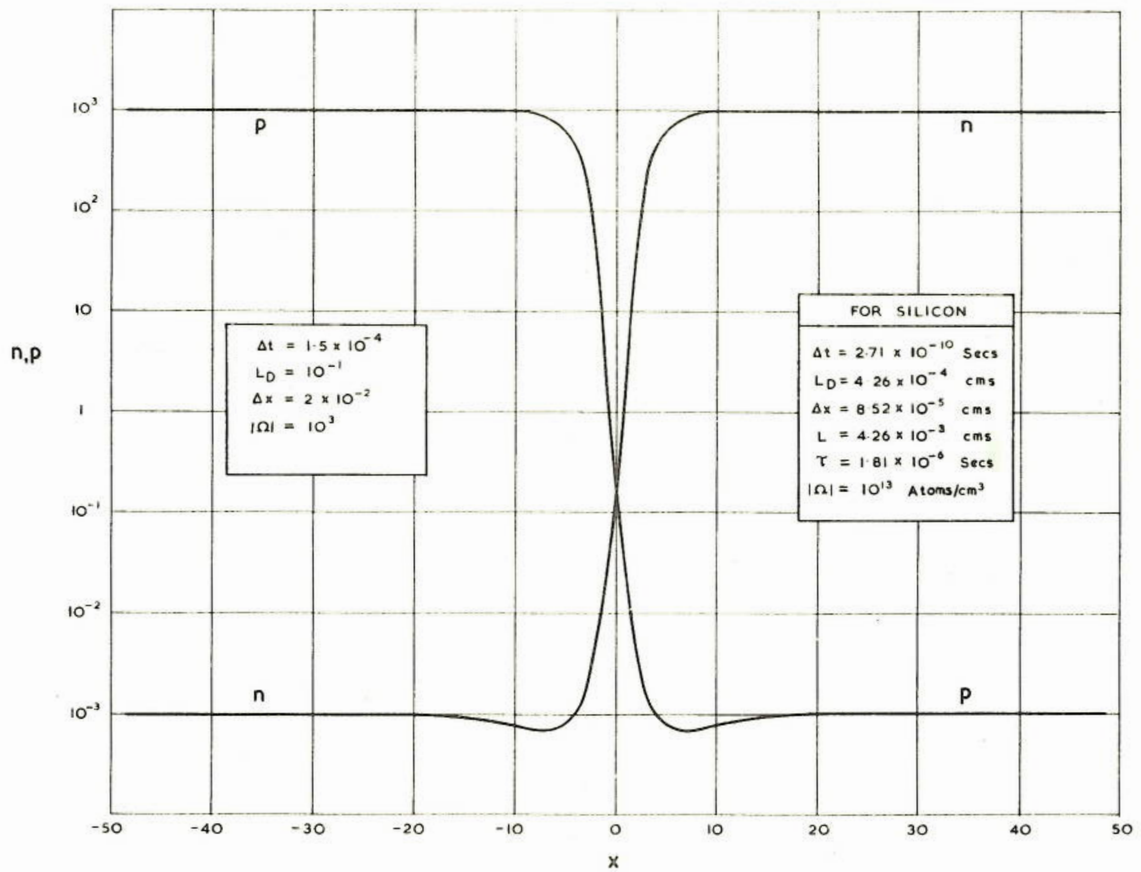

FIG. B1 ELECTRON AND HOLE DISTRIBUTION IN ABRUPT SYMMETRIC P-N JUNCTION AT A FORWARD ELECTROSTATIC POTENTIAL DIFFERENCE OF 11·8155

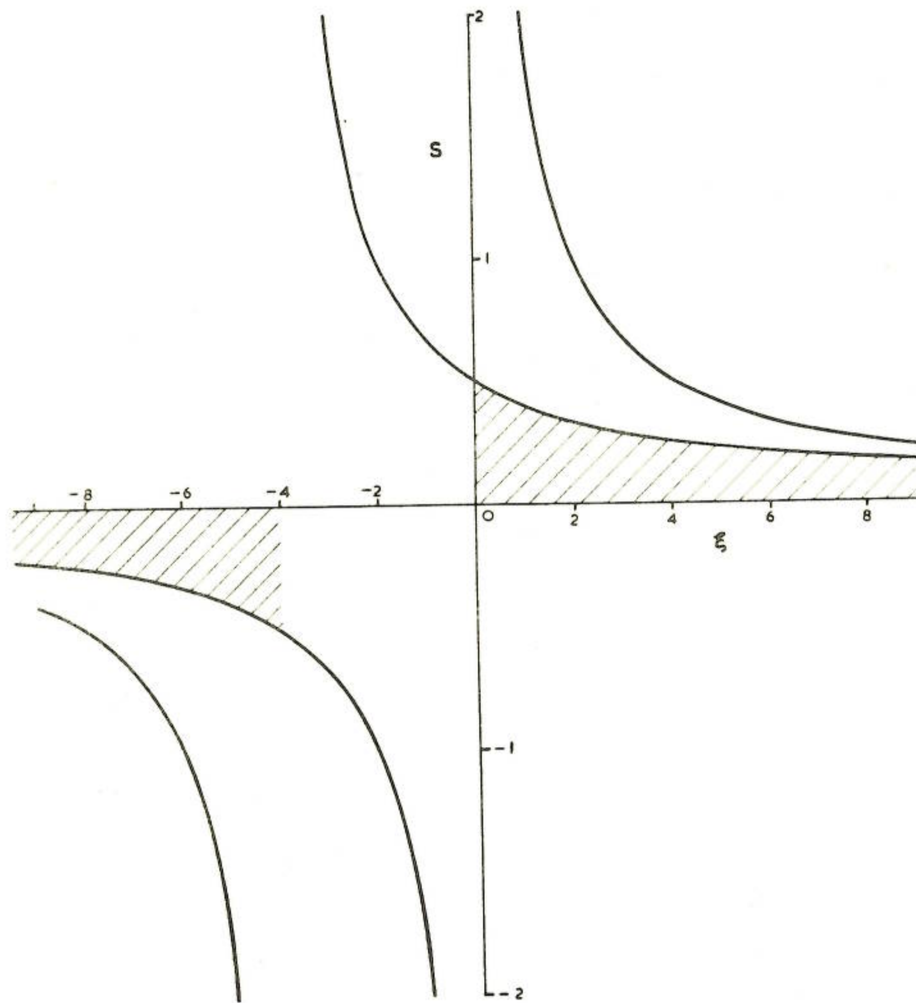

FIG. B2 REGION OF ξ-STABILITY (SHADED)

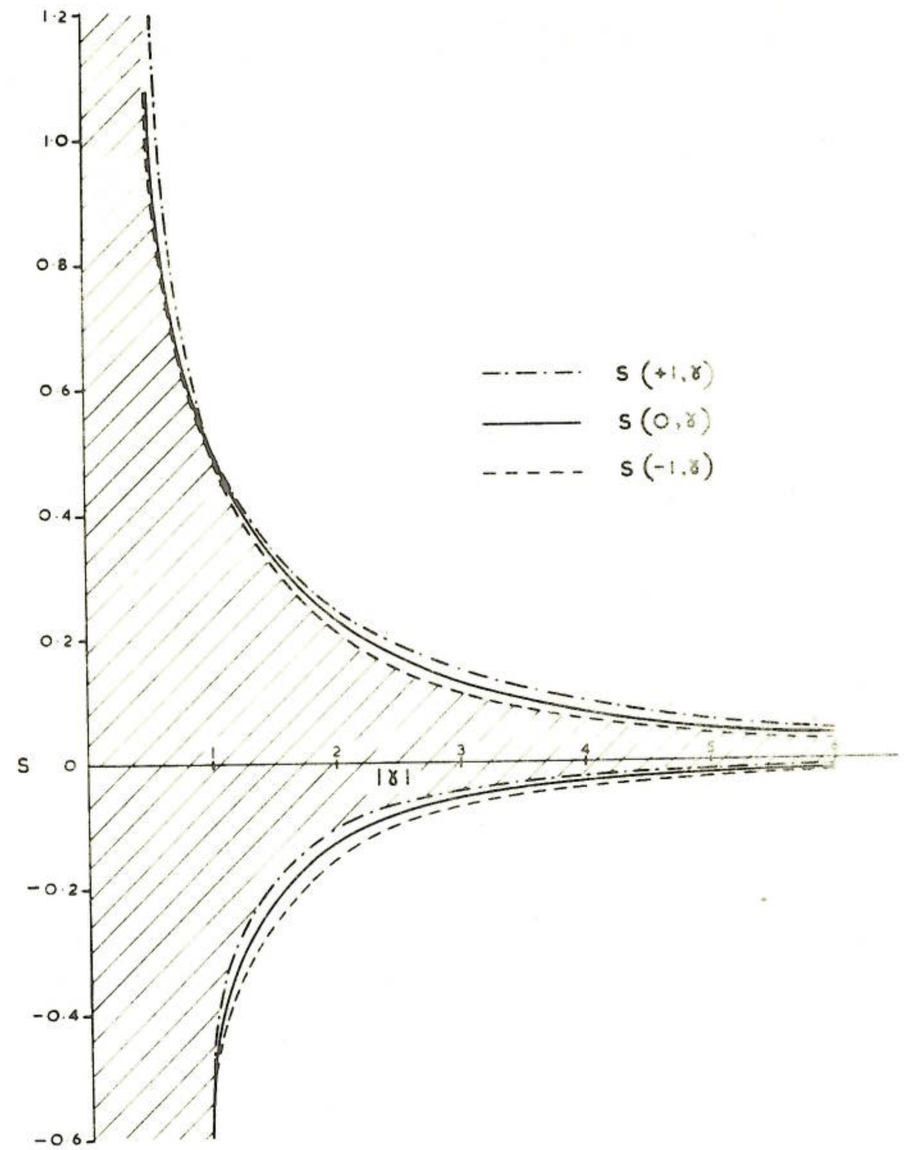

FIG. B3 REGION OF γ-STABILITY (SHADED)